Renewable and Sustainable Energy Reviews 52 (2015) 400–417

Contents lists available at ScienceDirect

Renewable and Sustainable Energy Reviews

journal homepage: www.elsevier.com/locate/rser

Modeling of photovoltaic system for uniform and non-uniform irradiance: A critical review

Debashisha Jena*, Vanjari Venkata Ramana

National Institute of Technology Karnataka, Surathkal, Mangalore 575025, India

ARTICLE INFO

Article history:
Received 1 July 2014
Received in revised form
14 May 2015
Accepted 11 July 2015
Available online 14 August 2015

Keywords:
Modeling
Uniform irradiance
Non-uniform irradiance
Photovoltaic (PV) array

ABSTRACT

A critical review on various modeling approaches of photovoltaic array both under uniform and non-uniform irradiance is presented in this paper. The main approaches that have been deliberated are based on the variation of analytical methods, classical optimization techniques and soft computing techniques. The review has been taken from papers published up to 2015. In this paper a detailed description and classifications of modeling techniques for both uniform and non-uniform irradiance conditions are presented. Modeling of PV systems under uniform irradiance is classified into non-iterative methods, iterative methods, artificial intelligence based methods and dynamic models. Under non-uniform irradiance, they are classified into non-iterative methods, iterative methods and artificial intelligence based methods. It is envisaged that this paper can serve as valuable information for researchers to work on photovoltaic array modeling under partial shaded condition.

Contents

* Corresponding author.
E-mail addresses: bapu4002@gmail.com (D. Jena), venkat.vr90@gmail.com (V.V. Ramana).

http://dx.doi.org/10.1016/j.rser.2015.07.079
1364-0321/

1. Introduction

Photovoltaic (PV) system directly converts sunlight into electricity. The fundamental device in a photovoltaic system is the photovoltaic cell. Mono-crystalline silicon, multi-crystalline silicon, amorphous silicon, cadmium telluride, copper indium and gallium sulfide, etc. are presently employed in manufacturing a photovoltaic cell. A photovoltaic cell is a semiconductor diode whose p–n junction is exposed to light. The light incident on the photovoltaic cell generates charge carriers that produce electric current. A single cell can produce around 0.7 V DC. So the PV cells are arranged in series to form modules. Modules are connected in series or parallel to form panels and group of panels constitute an array [1].

The PV model takes the temperature (T) and irradiance (G) as input and produces the electrical parameters of the equivalent circuit model as output. There are different types of equivalent circuit models viz., single diode model, two diode model, dynamic model, etc. The electrical parameters of single diode equivalent circuit are photovoltaic current or light generated current (I_{ph}), reverse saturation current of diode (I_o), diode ideality factor (a), series resistance (R_s) and shunt resistance (R_p). These parameters are to be accurately determined for modeling a photovoltaic source. A single diode model is shown in Fig. 1.

By applying KCL to Fig. 1, Eq. (1) is obtained.

$$I = I_{ph} - I_o\left[\exp\left(\frac{q(V+IR_s)}{akTN_s}\right)-1\right]-\frac{V+IR_s}{R_p} \quad (1)$$

Fig. 2 represents a double diode model. In this model an extra diode is connected anti-parallel to current source which represents the recombination losses in the depletion region.

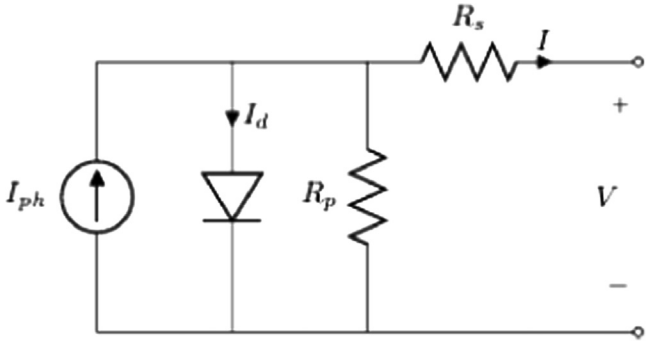

Fig. 1. Single diode model.

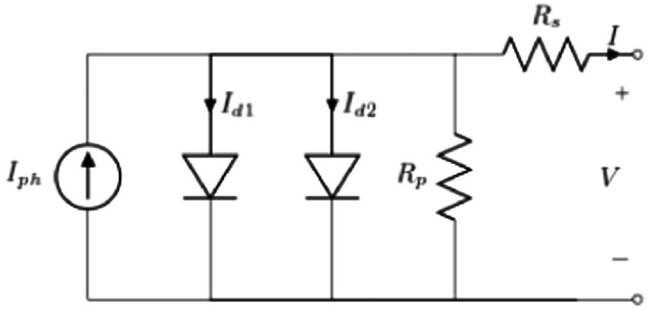

Fig. 2. Two diode model.

By applying KCL to Fig. 2, Eq. (2) is obtained.

$$I = I_{ph} - I_{o1}\left[\exp\left(\frac{q(V+IR_s)}{a_1kTN_s}\right)-1\right]- I_{o2}\left[\exp\left(\frac{q(V+IR_s)}{a_2kTN_s}\right)-1\right]-\frac{V+IR_s}{R_p} \quad (2)$$

In addition to the parameters in single diode model, the reverse saturation current (I_{o2}) and diode ideality factor (a_2) are the extra parameters that are to be calculated from two-diode model [1].

In some models the value of shunt resistance is neglected and it is known as R_s model. Eq. (3) represents R_s model.

$$I = I_{ph} - I_0\left[\exp\left(\frac{q(V+IR_s)}{akTN_s}\right)-1\right] \quad (3)$$

In some cases both series and shunt resistance are neglected and the model is termed as ideal diode model. A three diode model is presented in [2]. Apart from these models there are explicit models and dynamic models. Explicit models do not require an equivalent circuit for obtaining the output voltage and output current. In order to investigate the situations like resonance on DC cables, interaction of PV array with switching frequency harmonics and under damped currents, dynamic model is developed with inductor and capacitor [125]. Apart from the forward bias characteristics, reverse bias and dynamic characteristics will be obtained from dynamic model which are significant under non-uniform irradiance conditions. The equivalent circuit of dynamic model is presented in Fig. 3 [3].

PV modules are connected in series or parallel to form panels and panels are connected in series or parallel to form arrays. When part of PV array is subjected to conditions like shadows, PV array is subjected to non-uniform irradiance. The shaded modules limit the output current passing through unshaded modules. Shaded modules will dissipate heat and hotspots will be created. In order to avoid this, all the modules are connected with bypass diodes in anti-parallel providing alternate path for the output current [4].In order to obtain maximum output power from a PV source it is very important to obtain P–V characteristics under condition of non-uniform irradiance. The authors of the review paper presented in [5] have covered the papers published in between 1960 and 2011. Even though there are papers in 2011 and beyond, most of the methods covered up to 2008 and reviews only uniform irradiance conditions. The present paper includes a critical review ranging from 1969 to 2015 and discusses modeling in both uniform and non-uniform irradiance conditions. An attempt is made to compare the methods of modeling in uniform and non-uniform irradiance conditions. The methods in dynamic modeling are also included in this review.

This paper is organized as follows: Section 2 presents review on modeling uniform irradiance conditions. Section 3 presents modeling

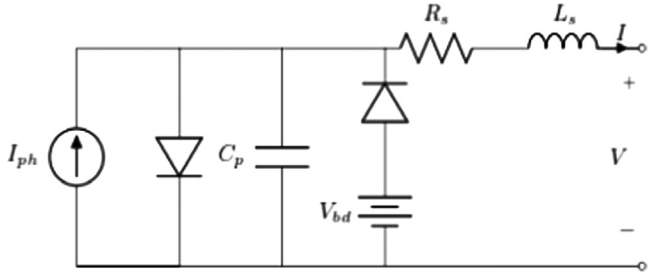

Fig. 3. Dynamic model [3].

Nomenclature

V_{ocn}	nominal open circuit voltage
I_{scn}	nominal short circuit current
I_{mp}	current at maximum power point
V_{mp}	voltage at maximum power point
P_m	maximum power
STC	standard test condition
T_n	cell temperature at STC
G_n	irradiance at STC
G	irradiance received by PV module
T	PV cell temperature
T_a	ambient temperature
K_v	voltage temperature coefficient
K_I	current temperature coefficient
N_s	number of cells in series in a module
N_{ss}	number of series modules connected
N_{pp}	number of parallel modules connected
V	output voltage of PV module
I	output current of PV module
V_{oc}	open circuit voltage at particular environmental condition
I_{sc}	short circuit current at particular environmental condition
OCC	open circuit condition
SCC	short circuit condition
MPP	maximum power point
I_{ph}	light generated current or photovoltaic current
I_o	reverse saturation current of diode (single diode model)
I_{o1}	reverse saturation current of diode 1 (two diode model)
I_{o2}	reverse saturation current of diode 2 (two diode model)
R_s	series resistance of PV module
R_p	parallel resistance of PV module
G_p	parallel conductance of PV module
a	ideality factor of diode (single diode model)
a_1	ideality factor of diode 1 (two diode model)
a_2	ideality factor of diode 2 (two diode model)
R_{so}	initial value of series resistance
R_{po}	initial value of shunt resistance
E_g	band gap energy
k	Boltzmann constant
q	electron charge
CC	co-content function
PLPB	Piecewise linear parallel branches model
SVD	singular value decomposition
RMSD	root mean square deviation
FF	fill factor
€	temperature coefficient of photovoltaic current
GA	genetic algorithm
PSO	particle swarm optimization
DE	differential evolution
CS	cuckoo search
ANN	artificial neural network
VO	vertical optimization
CF	curve fitting
CO	conductance optimization algorithm
L	series inductance
C_d	diffusion capacitance
C_j	junction capacitance
C_t	transition capacitance
C_B	breakdown capacitance
LSR	least square regression
SP	series parallel
TCT	total cross tied
BL	bridge linked
HB	honey bee
SS	simple series
INP	inflection point
POI	point of interest
DO	different oriented
PS	partial shading
BIPV	building integrated photovoltaic
ABC	artificial bee colony
LMA	Levenberg–Marquadt algorithm
NR	Newton–Raphson
IPM	interior point method
ANFIS	adaptive neuro-fuzzy interface system
RBFNN	radial basis function neural network
BMA	bird mating algorithm
TLBO	teaching learning based optimization
ABC	artificial bee colony

on non-uniform irradiance conditions. Section 4 presents the comparison of uniform and non-uniform irradiance conditions separately. Concluding remarks are presented in Section 5.

2. Review on uniform irradiance

Different approaches for equivalent circuit models of PV source under uniform irradiance are broadly classified into the following.

1. Non-iterative methods
2. Iterative methods
3. Artificial intelligence based methods
4. Dynamic models

2.1. Non-iterative methods

A single diode model is presented in [6] for calculating the values of equivalent circuit parameters. The parameters are calculated by substituting OCC, SCC and MPP in Eq. (1). Upon substituting, Eqs. (4)–(6) are obtained.

$$0 = I_{ph} - I_o\left[\exp\left(\frac{qV_{ocn}}{akTN_s}\right) - 1\right] - \frac{V_{ocn}}{R_p} \tag{4}$$

$$I_{scn} = I_{ph} - I_o\left[\exp\left(\frac{q(I_{scn}R_s)}{akTN_s}\right) - 1\right] - \frac{I_{scn}R_s}{R_p} \tag{5}$$

$$I_{mp} = I_{ph} - I_o\left[\exp\left(\frac{q(V_{mp}+I_{mp}R_s)}{akTN_s}\right) - 1\right] - \frac{V_{mp}+I_{mp}R_s}{R_p} \tag{6}$$

The values of series resistances and shunt resistances are calculated using their respective initial conditions, R_{so} and R_{po} which are deduced using Eqs. (7) and (8)

$$R_{so} = -\left(\frac{dV}{dI}\right)_{V=V_{oc}} \tag{7}$$

$$R_{po} = -\left(\frac{dV}{dI}\right)_{I=I_{sc}} \tag{8}$$

The value of diode ideality factor is obtained using

$$a_1 = \frac{V_{mpp} + I_{mpp}R_{so} - V_{oc}}{V_T\left[\ln\left(I_{sc} - \frac{V_{mp}}{R_p} - I_{mp}\right) - \ln\left(I_{sc} - \frac{V_{oc}}{R_p}\right)\left(\frac{I_{mp}}{I_{sc} - \frac{V_{oc}}{R_{po}}}\right)\right]} \tag{9}$$

The authors in [7] presented the work of [6] and additionally presented the parameters of two diode model. As in case of [6], the parameters are calculated using datasheet parameters, R_{so} and R_{po}. The conditions of OCC, SCC and MPP are substituted in Eq. (2) for obtaining Eqs. (10)–(12).

$$0 = I_{ph} - I_{o1}\left[\exp\left(\frac{qV_{ocn}}{a_1 kTN_s}\right) - 1\right] - I_{o2}\left[\exp\left(\frac{qV_{ocn}}{a_2 kTN_s}\right) - 1\right] - \frac{V_{ocn}}{R_p} \tag{10}$$

$$I_{scn} = I_{ph} - I_{o1}\left[\exp\left(\frac{q(I_{scn}R_s)}{a_1 kTN_s}\right) - 1\right] - I_{o2}\left[\exp\left(\frac{q(I_{scn}R_s)}{a_2 kTN_s}\right) - 1\right] - \frac{I_{scn}R_s}{R_p} \tag{11}$$

$$I_{mp} = I_{ph} - I_{o1}\left[\exp\left(\frac{q(V_{mp} + I_{mp}R_s)}{a_1 kTN_s}\right) - 1\right] - I_{o2}\left[\exp\left(\frac{q(V_{mp} + I_{mp}R_s)}{a_2 kTN_s}\right) - 1\right] - \frac{V_{mp} + I_{mp}R_s}{R_p} \tag{12}$$

Above equations are rearranged using the value of R_{so} and R_{po}. The value of R_s is calculated using quadratic and cubic solutions. Other parameters are calculated using the rearranged equations.

A method is presented in [8] for calculating the equivalent circuit parameters of R_s models using the datasheet values. The effect of temperature and irradiance on all model parameters and the cubic dependence of reverse saturation current on temperature are discussed. A similar method is implemented in [9] in which a generalized model is implemented in MATLAB-Simulink. The value of I_{ph} is approximated as I_{sc}. The diode reverse saturation is calculated in a similar manner as explained in [8]. It is reported that the change in the value of band gap energy E_g is based on the semiconductor used in manufacturing the solar cell. The diode ideality factor a, is selected in the range of 1–5 depending on the type of PV technology.

A method to extract the parameters using Lambert-W function is presented in [10]. A method to find diode ideality factor using Lambert-W-function is presented in [11]. The basic PV equation is rearranged by expressing PV current as explicit function of PV output voltage. Once four equivalent circuit parameters viz., I_{ph}, I_o, R_s, R_p are known, an explicit relation between a and I is obtained and the condition of OCC is substituted for determining the value of a. An explicit method to extract parameters is presented in [12]. For obtaining the equivalent circuit parameters Eqs. (4)–(6), (13) and (14) are considered. Similar to [12], the authors obtained the value of I_o, I_{ph} and R_p explicitly in [13].

$$\left.\frac{dP}{dV}\right|_{P=P_m} = \frac{d(I_m V_m)}{dV} = I_m + V_m \left.\frac{dI}{dV}\right|_{P=P_m} = I_m + V_m\left[\frac{-(I_{sc}R_p - V_{oc} + I_{sc}R_s)e^{\frac{I_{sc}R_s - V_{oc}}{N_s V_t}} - \frac{1}{R_p}}{1 + \frac{(I_{sc}R_p - V_{oc} + I_{sc}R_s)e^{\frac{I_{sc}R_s - V_{oc}}{N_s V_t}}}{N_s V_t R_p} + \frac{R_s}{R_p}}\right] = 0 \tag{13}$$

$$-\left.\frac{1}{R_p}\right|_{I=Isc} = \frac{-(I_{sc}R_p - V_{oc} + I_{sc}R_s)e^{\frac{I_{sc}R_s - V_{oc}}{N_s V_t}} - \frac{1}{R_p}}{1 + \frac{(I_{sc}R_p - V_{oc} + I_{sc}R_s)e^{\frac{I_{sc}R_s - V_{oc}}{N_s V_t}}}{N_s V_t R_p} + \frac{R_s}{R_p}} \tag{14}$$

A method using the datasheet values and semi-empirical equations is presented in [14]. The reference values of parameters are obtained using the equations at OCC, SCC, MPP mentioned in Eqs. (4)–(6) at STC. The value obtained by equating dP/dV to 0 is presented in Eq. (13).The reference values obtained are altered based on values of irradiance and temperature. The parameter values varied based on G and T are a, I_o, I_{ph}, R_s, R_p, E_g. The work in [14] is limited to series connected PV cells. In [15] modified version of [14] is presented by extending the work to parallel connection of modules so that simulation is done for series and parallel connected modules together.

A circuit based simulation is presented in [16] in which the diode in single diode model is replaced by three parallel diodes. They are modeled in a piecewise linear manner using voltage sources, resistor and a diode in series for switching. Similar equivalent circuit is presented in [17] for 'k' branches. The diode characteristics are using 2^h line segments, where h is a whole number. The number of resistances is equal to 2^h which is calculated using the slope (m) of line segments and are computed according to

$$R_1 = \frac{1}{m_1}; \quad R_k = \frac{1}{m_k - m_{k-1}} \quad \text{for } k \geq 2 \tag{15}$$

The voltage sources termed as corner are equal to (2^h–1) since the corner voltage of first line segment is 0. An equal area method is used to find the corner voltages.

A simplified expression of Eq. (3) is given in [18] where the output voltage (V) is expressed as a function of output current (I), V_{mp}, I_{mp}, I_{sc}, C_1 and C_2 as shown in Eq. (16). C_1 and C_2 are coefficients given in Eqs. (17) and (18), respectively.

$$I = I_{sc}\left[1 - C_1\left(\exp\left(\frac{V}{C_2 V_{oc}}\right) - 1\right)\right] \tag{16}$$

$$C_1 = \left(1 - \frac{I_{mp}}{I_{sc}}\right)\exp\left(\frac{-V_{mp}}{C_2 V_{oc}}\right) \tag{17}$$

$$C_2 = \frac{\frac{V_{mp}}{V_{oc}} - 1}{\ln\left(1 - \frac{I_{mp}}{I_{sc}}\right)} \tag{18}$$

In [18] the effect of aging on PV panels is introduced by using a series and shunt resistance and this model is expressed as Norton's equivalent circuit in [19].

An explicit method of modeling photovoltaic module is presented in [20,21]. Using the explicit method there is no need to calculate the equivalent circuit parameters. The values of voltage, current and power are computed based on values of irradiance and temperature by using an explicit expression [20]. The model is validated at maximum power point. The explicit equation is given in Eq. (19) [21].

$$I = I_{ph} + z(T - 25) - \frac{e^{\cdot[V + w(25 - T_c)]} - 1}{e^m - 1} \tag{19}$$

where I is p.u. current referred to I_{sc}, I_{ph} is p.u. irradiance referred to 1000 W/m^2, m is an exponential factor, w is the voltage temperature coefficient referred to V_{oc}, and z is the current temperature coefficient referred to I_{sc}. I_{ph} is represented as irradiance in [21].

A method based on outdoor measurement and a mathematical formulation is developed for calculating the reference values of equivalent circuit parameters of single diode model [22]. Initially Eqs. (6)–(8) and (13) are obtained at OCC, SCC, and MPP. Then dV/dI at OCC and SCC are equated to negatives of R_s and R_p and taken as initial values and termed as R_{so} and R_{po}. These initial values of resistances are evaluated using the manufacturer's datasheet. By using the mathematical equations and several outdoor measurements four reference values viz., V_{ocn}, I_{scn}, I_{mpn}, V_{mpn} are calculated. These four reference parameters are used for calculating the rest of equivalent circuit parameters reference values. Once all the reference values are found then for a specified environmental condition, G and T effects are included in the

particular equation and the equivalent circuit parameters are calculated at that environmental condition.

An ideal diode model is presented in [23]. The equations are taken at OCC, SCC, MPP and the equivalent circuit parameters viz., I_{ph}, I_o and a are calculated. The effects of environmental conditions, G and T on equivalent circuit parameters are included in this paper [23]. This method is used for simulating large array simulations.

A two diode model is presented in [24]. Values of R_s and R_p are calculated by differentiating voltage with respect to current at open circuit and short circuit current, respectively. The values of diode currents are calculated by using the following equations:

$$I_{d1} \approx CaT^3 \exp\left(-\frac{E_g(T)}{kT}\right) \tag{20}$$

$$I_{d2} = \frac{1}{\beta}\left(\frac{V_{oc} - I_{sc}R_s}{R_{so} - R_s} - I_{sc} - \alpha I_{d1}\right) \tag{21}$$

Ideality factor of second diode is selected to 2. Ideality factor of diode 1 is calculated according to Eq. (9).

A generalized PV model presented in [25] is implemented in PSCAD. The values of a, R_s, R_p are calculated without any iteration method. They are calculated at OCC, SCC, MPP, $dP/dV=0$ using Eqs. (4)–(6) and (13). Mainly the R_p is calculated based on Eq. (22) by replacing J with I.

$$\left.\frac{dJ}{dV}\right|_{V=V_{mp}} = -\frac{J_{mp}}{V_{mp}} \tag{22}$$

The values of I_{ph} and I_o are calculated based on other three equivalent circuit parameters.

The value of light generated current is calculated by taking the effect of temperature and irradiance. A single diode model that computes five parameters analytically is presented in [26]. This method uses five equations to compute the equivalent circuit parameters. The five equations are obtained at OCC, SCC, dI/dV at OCC and SCC, and $dP/dV=0$. It is difficult to find dI/dV at $V=0$ and $I=0$. In order to avoid this problem a four-parameter model is developed based on mathematical equation neglecting R_p. From the simplified equations, the four parameters of R_s model are calculated. By using these four parameters, dI/dV at $V=0$ and $I=0$ are calculated. By solving the equations at different environmental conditions, the parameters are calculated for any value of G and T. Finally all the obtained parameters are substituted in Eq. (1) to get accurate curve fitting.

The parameters are calculated with huge mathematical computations and are expressed as explicit functions of datasheet values, R_{so} and R_{po}. A rigorous mathematical study of model is performed in [27] to obtain the geometrical properties of single diode model. Once properties are obtained with the help of experimental values of I and V, the module parameters are calculated in a simplified manner. An improvement in R_s model is presented in [28] where the open circuit voltage and voltage at maximum power are corrected based on environmental conditions to obtain the accurate results. Then the equivalent circuit parameters are calculated (Table 1).

2.2. Iterative methods

The equivalent circuit parameters of CdS solar cell using a single diode model is presented in [29]. Model parameters are calculated using Eqs. (4)–(6), and (13) at OCC, SCC, MPP, respectively and dI/dV at OCC and SCC. All the equations are solved using Newton–Raphson method for obtaining the equivalent circuit parameters. The effect of temperature is not considered in the modeling process.

A method based on Newton model using a non-linear least square algorithm is presented in [30]. A Levenberg parameter is

Table 1
Comparison of non-iterative methods.

#	Authors	Ref.	Type	Par.	Contribution
1	Phang et al. (1984)	[6]	1D	5	Calculated based on equations at OCC, SCC, MPP
2	Chan et al. (1987)	[7]	2D	7	R_s is calculated using spline and cubic methods. Others parameters are calculated based on OCC, SCC, and MPP
3	Walker et al. (2001)	[8]	R_s	4	Calculated analytically using temperature effects
4	Tsai et al. (2008)	[9]	R_s	4	Extended [8] by incorporating E_g in calculation
5	Jain et al. (2004)	[10]	1D	5	Used Lambert-W function
6	Jain et al. (2005)	[11]	1D	5	Used Lambert-W function
7	Cubas et al. (2014)	[12]	1D	5	I_{ph}, I_o, R_p are expressed explicitly normally. R_s is in an implicit equation. It is expressed explicitly using lambert-W function and parameters are calculated
8	Cubas et al. (2014)	[13]	1D	5	Extension of [12], but R_s is calculated with huge mathematical computations using the values of R_{so} and R_{po}
9	De soto et al. (2006)	[14]	1D	5	Calculated using OCC, SCC, MPP and other points
10	Tian et al. (2012)	[15]	1D	5	Extended [14] to parallel connection
11	Azab et al. (2009)	[16]	1D	5	Piecewise diode model is used
12	Wang et al. (2011)	[17]	1D	5	PLPB model is used
13	Bellini et al. (2009)	[18]	R_s	4	Simplified basic equation using arbitrary constants. Estimated effect of aging using resistances
14	Chakrasali et al. (2013)	[19]	R_s	4	Simplified [18] by representing in Norton's equivalent circuit
15	MassiPavan et al. (2014)	[21]	NA	–	No equivalent circuit. Used for large array simulations
16	Saloux et al. (2011)	[20]	NA	–	
17	Chouder et al. (2012)	[22]	1D	5	Calculated using outdoor measurements and points at OCC, SCC, MPP
18	Xiao et al. (2013)	[23]	ID	3	Calculated using points at OCC, SCC, MPP
19	Di Vincenzo et al. (2013)	[24]	2D	4	Diode current calculated directly. a_2 is arbitrarily chosen. a_1 is calculated using a relation with equivalent circuit parameters
20	Rahman et al. (2014)	[25]	1D	5	Calculated R_s, R_p and a using rigorous mathematical calculations
21	Bai, J et al. (2014)	[26]	1D	5	Initially R_s model parameters are calculated. Obtained parameters are considered as approx. parameters and 1D parameters are calculated
22	Toledo et al. (2014)	[27]	1D	5	Calculated in simplified manner using geometrical properties of single diode model
23	Khezzar et al. (2014)	[28]	R_s	4	V_{oc} and V_{mp} are corrected based on environmental conditions for rapid convergence.

introduced for modification of non-linear least square algorithm. The problem formulation is given in Eq. (23).

$$S(P) = \sum_{i=1}^{N} [I_i - I_i(V_i, P)]^2 \tag{23}$$

In the above expression I_i is the measured value, I_i (V_i, P) is the simulated value, P (I_{ph}, I_o, R_s, G_{sh}, a) represents the parameters and N is the set of experimental data available.

A two diode model is implemented in [31]. Six equivalent circuit parameters viz., I_{ph}, I_{o1}, I_{o2}, R_s, R_p, a are computed. The model consists of a data acquisition system for collecting data of I and V and curve fitter to find the equivalent circuit parameters based on the value of G and T. Thirteen constants (K_0–K_{12}) are to be evaluated for each atmospheric condition using the curve fitter to calculate the values of equivalent circuit parameters accurately. Even though this method is accurate but it is highly complex. The process mentioned in [32] is similar to [31] but explained in an elaborate manner. Levenberg–Marquardt curve fitting technique is used to find the equivalent circuit parameters. In order to apply this curve fitting technique, initial values should be known. Calculation of initial values involves huge mathematical calculations which are to be solved iteratively. After the initial values are calculated the values of equivalent circuit parameters are calculated based on the values of irradiance and temperature. Similar work is carried out in [33]. Same procedure is followed in [34] and a new equation of E_g is presented which is given in Eq. (24).

$$E_g = N_s\left(1.16 - 7.02 \times 10^{-4} \cdot \frac{T^2}{T - 1108}\right) \tag{24}$$

A Levenberg–Marquardt algorithm (LMA) along with least square error criteria is used in [35] for finding the equivalent circuit parameters. A LMA in combination with SA is presented in [36]. An objective function is formulated and LM curve fitting is used to find the five equivalent circuit parameters. The simulated annealing approach is used to adjust the damping factor of LMA so as to increase the speed of the algorithm. In [37], voltage is expressed as an explicit function of current using arbitrary coefficients by performing mathematical computations. With the experimental data, LMA is used for extraction of parameters. In [38], LMA is used to extract the parameters from five different types of modules available in the literature.

A method based on LMA and Gauss algorithm is presented in [39]. Total six equations are obtained at OCC, SCC, MPP, dI/dV at I_{sc} and V_{oc}. Another equation is obtained by substituting temperature coefficient in voltage in Eq. (1). From the obtained six equations, five parameters are extracted using LMA. Gauss algorithm is used in conjunction with LMA so as to have a rapid convergence in estimating the parameters. The same model is used for performance prediction in [40].

A conductance optimization algorithm using a single diode model is proposed in [41]. Five equivalent circuit parameters need to be computed. The objective function to be minimized is same as Eq. (23). Here I_{ph} is not included in the optimization process. So, $P=(I_o, R_s, R_p, a)$ are the parameters to be calculated. Once these four parameters are computed, I_{ph} is found. In order to minimize the sum of squares, $dS/dX=0$ is solved, where X is the number of parameters. The initial values are calculated using a simplified conductance method. These initial values are entered into conductance optimization algorithm and final parameters that obtain the best fit are determined.

A method has been developed based on Lambert-W and co-content function in [42]. Single diode model is employed to find the parameters. The output current of PV array is expressed as an explicit function of other circuit parameters using Lambert-W function. Co-content (CC) function is applied to the explicit function and is reduced to purely algebraic form in terms of I, V, IV, V^2, I^2. The developed algebraic equation is fitted with experimental data to determine the model parameters.

The model proposed in [43] is a data based approach implemented using look-up table. This model is a single diode model termed as adaptive perturbation model with R_p neglected. Four parameters viz., I_{ph}, I_o, R_s, a are computed. As R_p is neglected Eq. (1) can be modified as given in Eq. (3). By substituting OCC, SCC, MPP in Eq. (3), Eqs. (25)–(27) are deduced, respectively.

$$0 = I_{ph} - I_o\left[\exp\left(\frac{qV_{ocn}}{akTN_s}\right) - 1\right] \tag{25}$$

$$I_{scn} = I_{ph} - I_o\left[\exp\left(\frac{q(I_{scn}R_s)}{akTN_s}\right) - 1\right] \tag{26}$$

$$I_{mp} = I_{ph} - I_o\left[\exp\left(\frac{q(V_{mp} + I_{mp}R_s)}{akTN_s}\right) - 1\right] \tag{27}$$

To include the temperature effects the values of (R_s, a) are varied at particular temperature until $\left(dI/dV|_{V=Vmpp} + (I_{mpp}/V_{mpp})\right)$ is minimized to a pre-specified tolerance limit. Then the optimal values of a and R_s are obtained at that particular environmental condition. This process is carried for different values of temperature. From the obtained values of a and R_s at different temperatures, two look-up tables are formed that are (T vs. R_s) and (T vs. a). The G and T effects are included for calculation of I_{ph} and I_o. Based on this a Simulink model is constructed that calculates the PV current for a given PV voltage.

In [44], an analytical method is used to calculate the equivalent circuit parameters of a single diode model. Eqs. (6), (13) and (14) are solved iteratively using a numerical approach to obtain the values of a, R_s, R_p. The calculated values R_s, R_p, a, are substituted in Eqs. (4) and (5) to find the values of I_{ph} and I_o. The authors in [45] have chosen Gauss Siedal method as a numerical approach to find the equivalent circuit parameters of single diode model and the method is similar to [44]. The principle of Gauss Siedal is expressed as in Eq. (28).

$$X^{k+1} = f\left(X^k\right) \tag{28}$$

A single diode model similar to [45] is implemented with few simplifications in [46]. The diode that represents recombination at quasi neutral region is approximated as piecewise liner model. The circuit formed is thus expressed in Thevenin's equivalent circuit form.

The method in [47] is an improvement of [44]. In [44] all the equivalent circuit parameters are computed without any initial guess. So the procedure to find the initial guess is discussed in [47]. The initial value of R_s is obtained by equating R_p to infinite and diode ideality factor as 1 as given in Eq. (29).

$$R_{so} = V_{oc} - \left[\frac{\ln\left[\frac{I_{ph} - I_{mp}}{I_o}\right] N_s V_t}{I_{mp}}\right] \tag{29}$$

The initial value of ideality factor is taken as the inverse of fill factor. The initial values of R_s and a are substituted in the equation of MPP to find the initial value of parallel resistance, R_{po}. Rest of the procedure for calculation of equivalent circuit parameters is same as [44].

The authors in [48] present a two diode model by substituting OCC, SCC, MPP, $dP/dV=0$, and $dI/dV=-1/R_p$ in Eq. (1). The equations are simplified and approximate solutions of the parameters viz., I_{ph}, I_{o1}, I_{o2}, R_s and R_p are obtained. These solutions serve as initial condition for numerical analysis and accurate parameters are obtained.

In [49] an ideal diode model is implemented with two empirical models. The equations are expressed at OCC, SCC and

MPP by making necessary approximations. Once the equations are obtained the parameters are calculated by fitting the experimental values with an optimization algorithm. The models are implemented in Mathcad.

An analytical method is presented in [1] based on single diode model. Four equivalent circuit parameters viz., I_{ph}, I_o, R_s, R_p are determined. The value of diode ideality factor is selected arbitrarily. The authors used a power matching algorithm where the maximum power value given in the datasheet ($P_{m,e}$) is made equal to maximum power obtained during simulation ($P_{m,m}$) and an equation for R_p is deduced as given in Eq. (30).

$$R_p = V_{mp}(V_{mp}+I_{mp}R_s)/\left\{V_{mp}I_{pv}-V_{mp}I_o\exp\left[\frac{q(V_{mp}+I_{mp}R_s)}{akTN_s}\right] + V_{mp}I_o - P_{m,e}\right\} \quad (30)$$

The value of R_s is incremented and the corresponding value of R_p is found, until $P_{m,e}=P_{m,m}$. When the condition is satisfied the value of (R_s, R_p) is considered as final value. The values of I_{ph} and I_o are calculated from the obtained values of R_s, R_p, a based on temperature and irradiance. A two diode model is implemented in [50] which is extension of single diode model in [1]. Four parameters I_{ph}, I_o, R_s, R_p are calculated. The reverse saturation of both the diodes is considered same. The diode ideality factor of diode 1 is considered as unity and that of diode 2 is taken as any value greater than 1.2 according to Schokley diffusion theory. Other parameters are calculated in a similar procedure to [1]. A simulator based on this method has been developed in [51] using MATLAB-Simulink.

The method proposed in [52] is the combination of the models discussed in [18,1]. The equations of OCC and SCC are presented in Eqs. (6) and (7). The values of R_s and R_p are calculated using a power matching algorithm as presented in [1]. In [52] the value of R_s is incremented adaptively that is based on error value. Error is the difference between datasheet maximum power and simulated maximum power. The value of diode ideality factor is selected arbitrarily. The idea of [1] is used in [53] which is an ideal two diode model (R_s and R_p neglected).

A method to extract the values of R_s and R_p is presented in [54] using Lambert-W function and Newton Raphson (NR) method. In [55], Eq. (1) is explicitly expressed using Lambert-W function as in [10] and Newton Raphson is used for extraction of parameters. In [56], similar method is employed but additionally the effects of temperature on parameters are incorporated. A method based on spline interpolation and bisection method is proposed in [57]. R_s model is used for modeling. Initially the I–V equation is expressed explicitly by using Lambert-W function. Natural cubic interpolation method is used to determine the values of I and P for corresponding values of V. Bisection method is used as an optimization method in determining the values of V that can produce maximum power.

A method based on pattern search is presented in [58,59] for extraction of parameters of single and two diode models by formulating an objective function.

A single variable optimization is presented in [60] for extracting parameters of single diode model. This method is generalized in [61] using numerical approaches. An explicit model is obtained using Lambert function in [62]. The effect of diode ideality factor on PV characteristics is studied. The parameters are extracted through an optimization algorithm.

A two diode model is developed based on singular value decomposition in [63] where the output voltage is dependent on irradiance, temperature and load voltage. SVD projects the problem on to a space described by orthogonal functions.

$$\text{Initially} \quad I_s = I_s(T,G,V_s) = \left|\overrightarrow{I_1}, \overrightarrow{I_2}, \ldots, \overrightarrow{I_q}\right| \quad (31)$$

Each value of I_i in the matrix represents a column vector. SVD is applied to the above equation.

$$I_s = UEV^T = \left|\overrightarrow{\phi_1(s)}, \overrightarrow{\phi_1(s)}, \ldots, \overrightarrow{\phi_p(s)}\right| \cdot A(T,G) \quad (32)$$

where U and V^T are orthogonal matrices, E is the diagonal matrix with singular values σ_1, σ_2….etc. These values are arranged in decreasing order such that $\sigma_1 \geq \sigma_2 \geq \ldots \sigma_l$, where l is the minimum of p and q. Each column I_j of I_s is expressed as linear combination of ϕ_k in uniform space. Whenever the value of σ_k becomes negligible, the computation will be performed up to that particular value of σ and the particular number is taken as r. $K > r$ is taken.

$$I_{s(i,j)} = \sum_{k=1}^{r}\left[a_k(T,G)_j\right]\ \varphi_k(i,j) \quad (33)$$

The values obtained from two diode model are compared with the SVD and a suitable fit is obtained.

A single diode model with reduced gradient optimization is presented in [64]. The reference value of I_{ph} is considered to be same as short circuit current. Four Eqs. (4)–(6), (13), (14) are taken at different operating conditions. In this method the authors choose R_p to vary independently. The value of R_p is found using a reduced gradient approach. Once the optimization begins, the other parameters are calculated and the value of R_p for which the best fit of I–V curve obtained is determined. With the obtained value of R_p after best fit, the other four equivalent circuit parameters are computed.

The five equations from Eqs. (4)–(6), (13), (14) are modified and rearranged in [65] to find the reference values of equivalent circuit parameters viz., I_{phn}, I_{on}, $R_{s,n}$, $G_{p,n}$. Algebraic modifications are done for all those five equations and two independent equations are formed with a and R_s to calculate the reference values of these two parameters. For solving a and R_s, an initial guess and boundary conditions need to be appropriately chosen. The boundary condition of a is [0.5, 2] as specified in most of the literature. The lower bound of R_s is considered as zero and the upper bound of R_s is given by

$$R_s^{max} = \frac{a_{ref}}{C_4}\left[1+W_{-1}\left(-e^{\frac{C_2-a_{ref}-2C_3}{a_{ref}}}\right)\right]+\frac{C_3}{C_4} \quad (34)$$

where $C_1 = \frac{K.T_n}{q}$, $C_2 = \frac{V_{ocn}}{N_s C_1}$, $C_3 = \frac{V_{mpn}}{N_s C_1}$, $C_4 = \frac{I_{mpn}}{N_p C_1}$.

The reference values of the rest I_{ph}, I_o, G_p are solved explicitly. In [66], a convex optimization algorithm is formulated for extraction of parameters using the reduced form of equations presented in [65]. A complete generalized analysis is carried in [67] both theoretically and practically.

A two diode model is presented in [68] and seven parameters are calculated. The equations are taken at OCC, SCC, MPP, from the voltage derivation at OCC, SCC and MPP. The seventh equation is obtained from diode ideality factor as arithmetic relation of a_1 and a_2. From these equations results are obtained using NR method. A method based on datasheet values is presented in [69]. Using Lambert-W function and three points on I–V curve, an iterative method with approximation is used for calculating the equivalent circuit parameters.

The authors in [70] have discussed an approach of parameter identification of diode model from the I–V curves of the PV panels in which the diode model is viewed as an equivalent output of a dynamic system.

A single diode model is presented in [71] where (4)–(6), (13), (14) are considered by replacing the current with current density (J). The light generated current is approximated as short circuit current. The

Table 2
Comparison of iterative methods.

#	Authors	Ref.	Type	Par.	Contribution
1	Kennerud et al. (1969)	[29]	1D	5	Calculated using OCC, SCC, MPP, dI/dV at OCC, SCC. Parameters are calculated by plotting characteristics for each parameters
2	Easwarakhanthan et al. (1986)	[30]	1D	5	Newton's method along LM algorithm is used
3	Gow et al. (1996)	[31]	2D	6	Curve fitting technique is used
4	Gow et al. (1999)	[32]	2D	13	Explained [31] in elaborate manner, LMA is used
5	Chowdhury et al. (2007)	[33]	2D	6	Similar to [32]
6	Nakanishi et al. (2000)	[34]	2D	6	Similar to [32], but E_g is considered
7	Gottschalg et al. (1999)	[35]	1D	5	LMA is used with least squared error
8	Dkhichi et al. (2014)	[36]	1D	5	LMA is used with simulated annealing
9	Bouzidi et al. (2007)	[37]	1D	5	LMA is used
10	Tossa et al. (2014)	[38]	1D	5	LMA is used for different algorithms
11	Ma et al. (2014a)	[39]	1D	5	Six equations are obtained to calculate five parameters. LMA is used
12	Ma et al. (2014b)	[40]	1D	5	Used [39] for performance prediction
13	Cheggar et al. (2004)	[41]	1D	5	Conductance optimization algorithm is used
14	Xiao et al. (2004)	[43]	R_s	4	Data-based approach using look-up tables
15	Ortiz-conde et al. (2006)	[42]	1D	5	Lambert-W function to express explicit function and co-content function is used for expressing the function for arbitrary values and optimization method is used to extract the variables
16	Sera et al. (2007)	[44]	1D	5	R_s, R_p and a are calculated iteratively using equations at OCC, SCC, MPP. I_{ph} and I_o are calculated analytically
17	Chatterjee et al. (2011a)	[45]	1D	5	Same as [44], iterative process performed using Gauss Siedal method
18	Chatterjee et al. (2011b)	[46]	1D	5	Diode in equivalent circuit is replaced by piecewise linear model
19	Can et al. (2014)	[47]	1D	5	Improved [44], by taking initial guess of R_s, R_p and a
20	Hejri et al. (2014)	[48]	2D	7	Eqs. (10)–(12) are used by simplifying them for equivalent circuit parameters
21	Petreus et al. (2008)	[49]	ID	3	Using any optimization technique
22	Villalva et al. (2009)	[1]	1D	4	Power matching algorithm by taking (R_s, R_p) a pair using Newton Raphson method. Rest of the parameters are calculated analytically
23	Ishaque et al. (2011a)	[50]	2D	4	Extended [1] for two diode model
24	Ishaque et al. (2011b)	[51]	2D	4	Implemented simulink version of [50]
25	Jena et al. (2015)	[52]	1D	4	Improved [1] by adaptively varying value of R_s
26	Babu et al. (2014)	[53]	2D	3	Same as [1] but (a_1 and a_2) are calculated using power matching algorithm
27	Ghani et al. (2011)	[54]	ID	5	Lambert-W function and Newton Raphson method
28	Ghani et al. (2014)	[55]	1D	5	Five parameters are obtained using basic equation and five experimental values of I and V
29	Ghani et al. (2015)	[56]	1D	5	Extended [55] by including temperature effects
30	Kong et al. (2012)	[57]	R_s	4	Spline interpolation and bisection method
31	AlHajari et al. (2012)	[58]	1D	5	Pattern search is used
32	AlRashid et al. (2011)	[59]	2D	7	Pattern search is used
33	Caracciolo et al. (2012)	[60]	1D	5	Single variable optimization
34	Camizzaro et al. (2014)	[61]	1D	5	Generalized model and numerical optimization is used
35	Xu et al. (2014)	[62]	1D	5	Effect of a on characteristics is studied
36	Zhang et al. (2013)	[63]	2D	7	Singular value decomposition
37	Mahmoud et al. (2013)	[64]	1D	5	Reduced gradient approach
38	Laudani et al. (2013)	[65]	1D	5	Solve a and R_s using optimization technique. Rest of the parameters are calculated analytically using a and R_s
39	Laudani et al. (2014a)	[66]	1D	5	A convex optimization problem is formed for calculating the parameters
40	Laudani et al. (2014b)	[67]	1D	5	Generalized analysis of [65,66]
41	Elbaset et al. (2014)	[68]	2D	7	Seven equations are obtained and NR method is used
42	Peng et al. (2014)	[69]	1D	5	Iterative method using three points on I–V curve and Lambert W function is used to express explicit relation
43	Lim et al. (2014)	[70]	1D	5	Linear system identification
44	Ding et al. (2014)	[71]	1D	5	Simplified work using arbitrary value K_{ref}
45	Lineykin et al. (2014)	[72]	1D	5	Calculated using OCC, SCC, MPP and $dP/dV=0$. a is selected arbitrarily

parameters R_s, and R_p are computed by utilizing Eqs. (22) and (35).

$$\left.\frac{dJ}{dV}\right|_{V=0} = -\frac{1}{R_p} \tag{35}$$

By using the values of R_s and R_p, the value of K_{ref} is calculated using Eq. (36).

$$K_{ref} = \sqrt[(V_{mpn}+R_sJ_{mpn}V_{ocn}-1)]{\frac{J_{scn}R_p - J_{mpn}R_p - J_{mpn}R_s - V_{mpn}}{J_{scn}R_p - V_{ocn}} - 1} \tag{36}$$

The irradiance and temperature dependence are taken into account in calculating the equivalent circuit parameters. An analytical single diode model is considered in [72] for modeling of the circuit. The equations are computed at open circuit condition, short circuit condition, maximum power point and $dP/dV=0$ as given in Eqs. (4)–(6), (13). There are four equation and five unknowns. So the diode ideality factor is considered to vary arbitrarily between 0.5 and 2 and is selected as independent variable, which is adjusted based on the divergence between the simulated and experimental curves. Then the rest four parameters are determined using the four equations. Apart from these two other parameters are computed i.e. band gap energy (E_g) and temperature coefficient of photo current (€). The values of E_g and € are calculated by using voltage and current temperature coefficients K_v and K_i that are mentioned in the manufacturers datasheet (Table 2).

Table 3
Comparison of GA methods.

#	Authors	Ref.	Type	Par.	Contribution
1	Moldovan et al. (2009)	[73]	1D	5	Crossing mate GA is used
2	Jervase et al. (2001)	[74]	2D	7	GA is used
3	Zagtouba et al. (2010)	[75]	1D	5	GA is used and validated using PASON cell tester
4	Lingyun et al. (2011)	[76]	1D	5	Adaptive GA with least square gradient is used
5	Ismail et al. (2013)	[77]	1D,2D	5,7	GA is used to calculate a, R_s, R_p as a decision vector using GA. Rest of the parameters are calculated analytically
6	Appelbaum et al. (2014)	[78]	1D	5	Similar to [77] but results are compared with NRM and LVM
7	Dizqah et al. (2014)	[79]	1D,2D	5,7	Based on GA and interior point method

Table 4
Comparison of PSO methods.

#	Authors	Ref.	Type	Par.	Contribution
1	Ye et al. (2009)	[80]	1D, 2D	5, 7	Conventional PSO without a good initial guess
2	Qin et al. (2011)	[81]	1D	5	Conventional PSO
3	Ye et al. (2010)	[82]	1D	5	An improved PSO with low value of objective function
4	Wei et al. (2011)	[83]	1D	5	PSO with chaos search
5	Macabebe et al. (2011)	[84]	2D	7	Dynamic inertia weight is added to conventional PSO
6	Sandrolini et al. (2010)	[85]	2D	7	PSO in conjunction with cluster analysis
7	Soon et al. (2012)	[86]	1D	5	PSO with inverse barrier constant
8	Hamid et al. (2013)	[87]	2D	7	Varying inertia weight and acceleration factor of conventional PSO
9	Khanna et al. (2015)	[88]	3D	8	Conventional PSO is used for three diode model
10	Soon et al. (2015)	[89]	Multi-dim.	Many	Multiple diodes are connected in series and parallel. Improved version of [86] (PSO with inverse barrier constant)

2.3. Artificial intelligence based methods

2.3.1. Genetic algorithm (GA)

A crossing mates GA technique is applied in [73] to find the equivalent circuit parameters of single diode model. The objective function formulation is done and explicit values of I obtained from simulation are compared with the experimental values for which the crossing mates GA is applied. In [74], a two diode model based on GA is presented where the parameter estimation is formulated as a search and optimized one. As it is necessary to have search range on parameters for applying GA, the approximate values are obtained through one of the conventional methods and accurate values are obtained by applying GA. A single diode model is considered in [75] to estimate the equivalent circuit parameters using GA. The results obtained through GA are validated using Pason cell tester. An adaptive GA with a least square gradient is used in [76] for adjustment of population size. This is done to enhance the performance of GA and reduce the influence of measurement error from experimental data. A global optimized GA that works for entire range is presented in [77] both for single and double diode models separately. A decision vector (a, R_s, R_p) is considered and calculated for entire range of values available in manufacturer's datasheet. Then necessary substitutions are made to find the values of I_{ph} and I_o based on particular values of irradiance and temperatures. A similar approach is followed in [78] where the results of GA are compared with NR method and LMA. A model based on GA and IPM is presented in [79] which formulates a multi-objective global optimization problem for Eq. (1) at STC and NOCT (Table 3).

2.3.2. Particle swarm optimization (PSO)

A conventional PSO is presented in [80] where PSO is used to obtain the parameters from the experimental data. PSO is applied to find the equivalent circuit parameters in [81] without any initial guess. An improved PSO is presented in [82] through which the parameters are obtained with more accuracy. A chaotic PSO is presented in [83] using chaos search that improves the global search performance and local convergence of PSO. The chaotic PSO also overcomes particle inertia and optimal parameters are searched without any limitations on search range. For improvement in performance a dynamic inertia weight function W^1 is used instead of W in [84]. The function is given by Eq. (37)

$$W^1 = WU^{-k} \tag{37}$$

The value of W varies between 0 and 1, U ranges in-between {1.0001–1.005} and k is the iteration number. PSO is used in conjunction with cluster analysis in [85]. Initially PSO is implemented to find the parameters. Once the results are obtained from PSO, cluster analysis is implemented to act as a correction filter for data obtained from PSO analysis. A PSO with inverse barrier constant is proposed in [86]. An objective function is formulated based on the values of OCC, SCC and MPP. The aim of this objective function is to find the optimum values of a, R_s and R_p. An inverse barrier function is formulated and incorporated into objective function which transforms the constrained optimization as an unconstrained problem. After the values of a, R_s and R_p are calculated, the values of I_{ph} and I_o are calculated. A method based on time varying inertia weight and acceleration factor of PSO is presented in [87]. A three diode model is proposed in [88], where the series resistance is made to vary linearly with load current and other parameters of model are calculated using PSO. A generalized PV model that allows adding diodes both in series and parallel in the equivalent circuit is presented in [89]. An improved version of [86] i.e., PSO with inverse barrier constant is presented to extract the parameters (Table 4).

2.3.3. Differential evolution (DE)

A method based on differential evolution is proposed in [90] where the values of series and shunt resistances change with temperature. There is no clear approach whether DE converges to global minima and there is no penalizing approach to ensure that the solution lies in feasible region [91]. In [92] the values of a, R_s, R_p for different environmental conditions are calculated using the information provided in the manufacturing datasheet. In [90] the parameters are determined using DE where the boundary conditions of the parameters are not specified. Two modified methods of

Table 5
Comparison of DE methods.

#	Authors	Ref.	Type	Par.	Contribution
1	da Costa et al. (2010)	[90]	1D	5	DE is used based on temperature value
2	Ishaque et al. (2012)	[91]	2D	7	Penalty based DE is used
3	Ishaque et al. (2011a)	[92]	1D	5	DE without boundary conditions is used and comparison is made with GA and PSO
4	Ishaque et al. (2011b)	[93]	2D	7	Two modified methods are presented – boundary based and penalty based
5	Gong et al. (2013)	[94]	1D	5	Rcr-JADE
6	Jiang et al. (2013)	[95]	1D	5	*F* and CR are varied based on fitness value

Table 6
Comparison of other EA methods.

#	Authors	Ref.	Type	Par.	Contribution
1	Asif et al. (2008)	[96]	1D	5	Simulated annealing using [110]
2	Naggar et al. (2012)	[97]	1D, 2D	5, 7	Simulated annealing
3	Ma et al. (2013)	[98]	1D	5	Cuckoo search
4	Siddiqui et al. (2013)	[99]	1D, 2D	5, 7	Hybrid EA – Tabu assisted DE, DE assisted Tabu, PSO assisted DE
5	Askazadeh et al. (2013a)	[100]	1D	5	Bird mating algorithm
6	Askazadeh et al. (2015)	[101]	1D	5	Simplified bird mating algorithm
7	Askazadeh et al. (2013b)	[102]	1D	5	Artificial bee swarm
8	Olive et al. (2014)	[103]	1D	5	Artificial bee swarm
9	Hasanien (2015)	[104]	1D	5	Frog leaping algorithm
10	Askazadeh et al. (2012)	[105]	1D	5	Harmony search
11	Han et al. (2014)	[106]	1D	5	Fish swarm optimization
12	Niu et al. (2014)	[107]	1D	5	Teaching lean based optimization (TLBO)
13	Patel et al. (2014)	[108]	1D	5	Simplified TLBO
14	Niu et al. (2014)	[109]	1D	5	Biogeography based algorithm

DE are presented in [93], i.e. boundary based DE and penalty based DE. Boundary based DE forces the PV parameters to be in a certain feasible region. Penalty based DE ensures the availability of model parameters in a feasible region. The method of extracting solar parameters using penalty based DE is also presented in [91]. An improved version of JADE is presented in [94] termed as Rcr-JADE. This is an adaptive DE in which crossover rate and ranking based mutation are proposed. In these two parameters, cross over rate (CR) and scaling factor (*F*) are adaptively varied. A ranking based mutation is presented that can accelerate the convergence of Rcr-JADE, thereby reducing computational effort. Another adaptive DE is presented in [95] in which the control parameters are adjusted automatically according to the fitness value during optimization process. The parameters varied are scaling factor (*F*) and crossover rate (CR). The fitness value of subsequent steps (i–1) and i are important factor in selecting the values of *F* and CR (Table 5).

2.3.4. Simulated annealing (SA)

A method is proposed based on simulated annealing in [96] for a single diode model with five parameters to be computed. The values of a and R_s are calculated using the manufacturer's datasheet at standard test conditions. The method overcomes the drawbacks of methods like GA viz., low speed, and high iterative fitness functions. The algorithm of this method is presented in [110]. The authors in [97] presented a variation in simulated annealing algorithm for extraction of PV parameters.

2.3.5. Cuckoo search

An evolutionary method for calculating the single diode equivalent circuit parameters is proposed in [98] using cuckoo search. The authors discussed the drawbacks of GA and PSO and addressed the advantages of this method. The values of resistances are calculated as in direct relation with irradiance.

2.3.6. Hybrid EA

Three types of hybrid evolutionary algorithms are presented in [99] to improve the performance than conventional evolutionary algorithms. The hybrid algorithms are (1) Tabu search assisted DE, (2) DE assisted Tabu search, and (3) PSO assisted DE. In all the cases the normalized error is expressed in terms of V_{oc}, I_{sc}, V_{mp}, I_{mp}.

2.3.7. Other EA

Other evolutionary algorithms for extraction of parameters are bird mating algorithm [100], simplified BMA [101] which reduces the parameter setting in original BMA, artificial bee swarm optimization [102,103], frog leaping algorithm [104], harmony search method [105], fish swarm optimization [106], TLBO [107], simplified TLBO [108], biogeography based optimization [109] (Table 6).

2.3.8. Neural networks, fuzzy and ANFIS

A fuzzy modeling approach is presented in [111] for a single diode model to compute the five equivalent circuit parameters. A regression fuzzy model is presented which is suitable for online applications and any type of PV system. A multi-layer feed forward network is used to find the equivalent circuit parameters in [112]. The input to the neural network is irradiance and temperature. Output is voltage and current. Two hidden layers are used. One hidden layer has six neurons (linear transfer function) and the other has 12 neurons (logsig transfer function). Levenberg Marquardt (LM) back propagation algorithm is used as training algorithm. Another method is presented using a three layer feed forward network in [113] using LM optimization algorithm. This method used two inputs, *G* and *T*. Five outputs are obtained which are the equivalent circuit parameters viz., I_{ph}, I_o, R_s, R_p, a. There are 20 hidden neurons. A generalized regression neural network is used in [114] to predict the operating current of photovoltaic module. The ANN based method presented in [115], generates *I–V* curves for any operating condition of mono-crystalline and poly-crystalline silicon solar cells. Multi-layer perceptron (MLP) is used

Table 7
Comparison of ANN methods.

#	Authors	Ref.	Type	Par.	Contribution
1	Elshatter et al. (2000)	[111]	1D	5	Fuzzy logic is used
2	Balzani et al. (2005)	[112]	1D	5	Four layer feed forward NN is used
3	Karapete eta al. (2006)	[113]	1D	5	Three layer feed forward NN is used
4	Celik et al. (2011)	[114]	1D	5	Generalized regression NN
5	Almonacid et al. (2009)	[115]	–	–	MLP with gradient descent approach. Generates *I–V* curve based on the values of *G* and *T*
6	Ramaprabha et al. (2009)	[117]	1D	5	Back propagation algorithm
7	Karamirad et al. (2013)	[116]	1D	4, 5	3:4:7:1 structure is used
8	Bonanno et al. (2012)	[118]	1D	5	RBFNN
9	Chikh et al. (2014)	[119]	ID	3	ANFIS
10	Fathabadi (2013)	[20]	1D	5	ANN with lambert-W function is used
11	Kulaksiz et al. (2013)	[21]	1D	5	ANFIS
12	Laudani et al. (2015)	[122]	1D	5	Hybrid ANN with I_{ph}, I_o, R_p reduced as explicit function of a and R_s. a and R_s are calculated analytically by NN. Rest are calculated analytically

Table 8
Comparison of dynamic models.

#	Authors	Ref.	Contribution
1	Madden et al. (1994)	[123]	Diffusion capacitance is calculated using frequency analysis
2	Kumar et al. (2005)	[124]	Diffusion and junction capacitance are modeled for Si solar cell
3	Kim et al. (2013)	[3]	Series inductance, diffusion, transition and breakdown capacitance are modeled using a DC sweep test and two AC frequency test
4	Di Piazza et al. (2013)	[125]	Series inductance and parasitic capacitance are calculated using least square regression algorithm

which is trained using a simple gradient descent based procedure. A multi-layer perceptron model is used to accurately predict the operating current and power of PV modules using back-propagation algorithm in [116,117]. In [116], a 3-4-7-1 topology is used where input consists of three neurons viz., *G*, *T* and output voltage. Among the two hidden layers, first hidden layer contains 4 neurons and the second hidden layer consists of 7 neurons. The output neuron is the panel current. A non-linear hyperbolic function is applied to produce the output. A radial basis function neural network (RBFNN) that gives superior performance than MLP is presented in [118]. This model predicts the value of current and power as a function of output voltage of corresponding circuit model at different values of *G*.

An ANFIS based model is presented in [119] that implements an ideal diode model. The input to the ANFIS is voltage and temperature and the output is current flowing through the diode. The architecture is 2:4:2:2:1 and I_{ph} is calculated analytically. A method based on combination of Lambert-W function and ANN is presented in [120]. A comparison is made between Lambert-W function of *I–V* characteristics with *I–V* relation of learned ANN. Another method of ANFIS is presented in [121] in which the inputs are V_{oc}, I_{sc}, type of PV material used and unit area below the *I–V* curve; the outputs are the equivalent circuit parameters. A hybrid NN is presented in [122] in which the I_{ph}, I_o, R_p are expressed as explicit functions of a and R_s in the reduced form. The neural network predicts the values of a and R_s and remaining parameters are calculated analytically using reduced form equations (Table 7).

2.4. Dynamic models

Dynamic models are the models with one dynamic variable either *L* or *C*. A diffusion capacitance model is discussed in [123], the value of which is measured using frequency analysis. A diffusion and junction capacitance model for si solar cell is given in [124], where the cells are tested at different temperatures to find the junction temperature. Dynamic models with more than one dynamic parameter are presented in this method. A comprehensive mathematical model is developed for dynamic model in [3] that includes forward bias, reverse bias and dynamical characteristics of PV array. The parameters in dynamic model viz., series inductance, diffusion, transition and breakdown capacitance are modeled. These values are obtained experimentally using a DC sweep test and two AC frequency tests. Another dynamic model to find the dynamic model parameters is proposed in [125] using least square regression algorithm. In this model, using time domain analysis a step load reference test is performed to separate the inductance and capacitance response on load current response. Dynamic model parameters are parasitic capacitance with series inductance. The proposed model reproduces the second order behavior of PV source (Table 8).

3. Review on non-uniform irradiance

3.1. Non-iterative methods

A complete model is presented in [4] in which the avalanche effect on a cell in reverse bias is described and the shading effects on a module are analyzed. Avalanche effect is presented in Eq. (38) which introduces a non-linear multiplication factor and it affects the current in shunt resistance.

$$I = I_{ph} - I_o\left[\exp\left(\frac{V+IR_s}{aV_t}\right)-1\right] - \left(\frac{V+IR_s}{R_p}\right)\varphi(V) \tag{38}$$

where

$$\varphi(V) = \left[1 + a\left(1 - \left(\frac{V+IR_s}{V_b}\right)^{-\beta}\right)\right] \tag{39}$$

The author avoided non-linear implicit equations governing PV cell circuits by sweeping the diode voltage and obtained the

corresponding *I–V* curves. An investigation on partial shading is done at module level in [127]. As it is a module level study no peaks and steps are detected in characteristics. An experimental study of mismatch shading effects is presented in [128,129]. Only module level study is performed and the effect of shading on complete PV array is not discussed. A model similar to [4] is used for modeling PV array under non-uniform irradiance in [130]. The conducting diode model is expressed explicitly using Lambert-W function. The negative voltage modeling part is expressed as a quadratic function [130]. An improved single diode model presented in [4] is used for modeling in [131]. The modeling process is extension of [132] where simplified expressions are developed and are implemented for generalized multi-string arrays. A method similar to [4] is implemented in [155] using linear approximation of bypass diode. The authors in [133] extended the work done in [4] to a two diode model. The equation is given in (40).

$$I = I_{ph} - I_{o1}\left[\exp\left(\frac{V+IR_s}{a_1 V_t}\right)-1\right] - I_{o2}\left[\exp\left(\frac{V+IR_s}{a_2 V_t}\right)-1\right] - \left(\frac{V+IR_s}{R_p}\right)\varphi(V) \tag{40}$$

This is done to know the working of solar cell in reverse bias region that include the effect of PV cell in reverse bias region and avalanche breakdown. Detailed model of bypass diode is considered. PSPICE simulation software is used. Apart from this the study of bypass diode configurations on PV modules is presented.

The authors in [134] extended the work in [8] for non-uniform irradiance. The entire array is divided into groups. Groups are divided into series assemblies. Series assemblies are divided into sub-assemblies. A sub-assembly is a group of modules receiving same insolation. Sub-assemblies are connected in series to form series assembly. Series assemblies having same shading pattern are connected in parallel to form a group. The model is implemented in MATLAB and has been experimentally validated. A MATLAB GUI is presented in [135] based on [134] for demonstrating the effect of partial shading using single diode model. A tool is developed in [136] based on [134] which included arbitrary cloud by using a sliding shading matrix. A combination of [18,134] is presented in [137].

An analytical modeling approach of partial shading is presented in [138] using single diode model. The temperature effect on reverse saturation is developed as cubic dependence [32] and the value of E_g is given by

$$E_g = 1.16 - 7.02\times10^{-4}\frac{T^2}{T^2+1108} \tag{41}$$

where T is the cell temperature given by

$$T = 273 + T_a + \left(\frac{NOCT-20}{0.8}\right)\frac{G}{1000} \tag{42}$$

Once the set of equations are modeled, three different cases are considered based on different oriented (DO) and partial shading (PS). DO is the general problem in BIPV. In the first case a different oriented module is considered in which two PV modules are connected in series with a bypass diode. The two modules receive different levels of insolation. In the second case, a single module is considered which consists of 36 cells in series with some cells shaded which is a case of partially shaded module. An extension of case 2 is presented in case 3, where two series PV modules protected by bypass diodes with some cells in one module are shaded. In all these three cases the model in the cell level has been extended to module level and necessary equations are deduced at that particular condition. The reverse voltage effect occurring in a module has been studied and modeled. The bypass diode in each case is modeled as piecewise linear.

The harmful effects of partial shading are presented in [139] and a PSPICE based simulation model is implemented to find the

Table 9
Comparison of non-iterative methods.

#	Authors	Ref.	Type	Par.	Diode	Contribution
1	Bishop (1988)	[4]	1D	7	D	Complete model including positive and negative characteristics
2	Kawamura et al. (2003)	[127]	1D	7	D	Module level study using [4]
3	Alonso-Garcia et al. (2006a)	[128]	1D	7	D	Experimental study
4	Alonso-Garcia et al. (2006b)	[129]	1D	7	D	Experimental study
5	Batzelis et al. (2014)	[130]	1D	7	D	Improvement of [4]. Positive part is modeled using Lambert-W function. Negative part using quadratic forms
6	Psarros et al. (2015)	[131]	1D	7	D	Improved model of [4]
7	Restrepo et al. (2013)	[155]	1D	7	P	Implemented [4] with linear approximation of bypass diode
8	Paraskevadaki et al. (2011)	[133]	2D	9	D	Extended [4] to a two diode model
9	Patel et al. (2008)	[134]	R_s	4	D	Modeled by dividing arrays into groups, assemblies and sub-assemblies
10	Bays et al. (2014)	[135]	1D	5	P	MATLAB GUI is developed for [134]
11	Paasch et al. (2014)	[136]	1D	5	P	Implemented [134] for a arbitrary cloud using a sliding sharing matrix
12	Yi et al. (2014)	[137]	1D	5	D	Implemented [134] using [18]
14	Wang et al. (2010)	[138]	1D	5	P	Implemented for DO and PS
15	Ramaprabha et al. (2008)	[139]	1D	5	P	Implemented using simulink
16	Ramaprabha et al. (2009)	[140]	1D	5	P	Implemented using simulink
17	Ramaprabha et al. (2010)	[141]	1D	5	P	Implemented using simulink
18	Ding et al. (2012)	[142]	R_s	4	P	Implemented using S-function builder in simulink
19	Aljami et al. (2013)	[143]	1D	5	D	Modeled based on different shading levels
20	MassiPavan et al. (2012)	[144]	–	–	–	Explicit model. Does not require models, used for long term forecasting
21	Di Vincenzo et al. (2013)	[24]	2D	7	D	Two diode model implemented using PSPICE
24	D'Alessandro et al. (2014)	[146]	–	–	BJT	BJT is used in place of bypass diode
25	Guo et al. (2012)	[147]	1D	5	D	Model dependent on time is developed
26	Gurrerre et al. (2014)	[148]	1D	5	P	Series connected modules are analyzed for partial shading
27	Lun et al. (2015)	[145]	1D	5	P	Method based on basic points on the *I–V* curve is proposed
28	Qi et al. (2014)	[149]	R_s	4	P	Extended [18] to non-uniform irradiance
29	Ollala et al. (2014)	[150]	R_s	4	P	Extended [18] to non-uniform irradiance by expressing voltage as a function of current
30	Rodrigo et al. (2013)	[151]	1D	5	P	Model in SP configuration is implemented
31	Torres et al. (2014)	[152]	1D	5	D	Dynamic thermal model along with single diode model is implemented
32	Khalid et al. (2014)	[153]	2D	7	D	Extended uniform irradiance model to non-uniform irradiance
33	Seyed mahmoudin et al. (2013)	[154]	1D	7	P	Analysis is carried out by considering with and without bypass diodes

D: detailed model of bypass diode; P: piece wise linear model of bypass diode;

type of connection that is less susceptible to shading effects. A similar type of work is done in [140,141] where three modules are connected in series and the effect of shading is analyzed. Bypass diodes modeled as piecewise linear model are connected across each module (sim power systems library of MATLAB implementation of a diode is piecewise linear model). An R_s model has been implemented in [142] to simulate the effects of non-uniform irradiance. The value of light generated current is approximated to short circuit current. The model is developed on MATLAB-Simulink using S-function builder and controlled current source. Initially block is constructed for uniform irradiance conditions. A C-Code is embedded in S-function builder where the process of obtaining array current is coded. These blocks are connected in series and parallel with bypass to analyze the effects of non-uniform irradiance.

A mathematical model based on single diode model is presented in [143]. The set of equations are described to obtain the *I–V* characteristics under non-uniform irradiance. Once the parameters are determined, Eq. (43) is used to obtain the *I–V* curve.

$$V=\begin{cases}\sum \frac{AkT}{q} n_s^{us} \ln\left(\frac{I_{sc}\lambda^{un}-I}{I_o}\right) & I > I_{Nstep}\\ \vdots & \\ \sum \frac{AkT}{q}\left(n_s^{us} \ln\left(\frac{I_{sc}\lambda^{un}-I}{I_o}\right)+n_s^{s1} \ln\left(\frac{I_{sc}\lambda^{s}-I}{I_o}\right)\right) & I_{1step} < I < I_{2step}\\ \sum \frac{AkT}{q}\left(n_s^{us} \ln\left(\frac{I_{sc}\lambda^{uN}-I}{I_o}\right)+n_s^{s1} \ln\left(\frac{I_{sc}\lambda^{uN}-I}{I_o}\right)+n_s^{sN} \ln\left(\frac{I_{sc}\lambda^{sN}-I}{I_o}\right)\right) & I < I_{step}\end{cases} \quad (43)$$

where n_s^{us} is the number of unshaded modules, n_s^{sN} is the number of partially shaded modules, λ^{uN} is the irradiance level in uniform irradiance condition, λ^{sN} is the highest irradiance level of partially shaded modules, *N* is the number of distributed irradiance levels. If there are *N* distributed irradiance levels there will be *N* steps in the *I–V* curve.

A study on the mismatch effect for large-scale solar parks is proposed in [144]. This is an explicit empirical model in which there is no need to find the equivalent circuit parameters. The presented method expresses PV current as a function of voltage. As this is a simplified model, this can be used to simulate the mismatch effect for large scale solar parks in a less time with a compromise in accuracy.

A detailed two diode model under non-uniform irradiance is presented in [24]. Ideal bypass diodes are considered and PSPICE simulation software is used for simulating the array in non-uniform irradiance conditions.

A BJT in saturation mode is used as a bypass diode in [146] instead of bypass diode. Under critical shading conditions the Schottky diode supports the BJT. In [147] a model dependent on time is developed for investigating the effects of moving shadows. Bypass diode configurations are studied in detail. It is implemented in LT SPICE. In [148] different modules are connected in series and effect of partial shading on all those modules is studied. A method based on OCC, SCC, voltage and current at MPP is used for extraction of model parameters in [145].

Authors in [167] have extended the idea of modeling presented in [18] for non-uniform irradiance conditions. A model similar to [18] is extended for non-uniform irradiance by expressing voltage as a function of current in [150]. An simplified model using SP configuration that does not require complete points on the *I–V* curve is presented in [151]. A dynamic thermal model along with a single diode model is presented in [152]. A two diode model is presented in [153] for calculating seven equivalent circuit parameters. The model is extended to non-uniform irradiance using a detailed model of bypass diode. A theoretical analysis under non-uniform irradiance is carried out in [154] by considering the effect with and without bypass diode (Table 9).

3.2. Iterative methods

A numerical simulation of *I–V* characteristics of PV cells under partial shading condition is proposed in [156]. To simulate *I–V* characteristics under partial shaded condition, each individual cell is modeled using a numerical algorithm. All the elements of PV cell and blocking and bypass diodes are expressed in terms of complex mathematical expressions. Although it is complex, it provides accurate results. A method based on this model is proposed in [157] where the work is extended to various configurations like SP and TCT, implemented in MATLAB.

The model presented in [158] is extension of work done in [50,51]. The non-uniform irradiance model is obtained by taking the effect of array configuration, shading pattern, *G* and *T*. A linear interpolation with extrapolation techniques are used to find the *I–V* and *P–V* characteristics under non-uniform irradiance conditions. A 20×3 array is considered for simulating the effect of non-uniform irradiance. A MATLAB-Simulink based PV simulator is presented in [159]. In this a 20×3 array four shading patterns are considered.

The model based on field measurements is presented in [160]. Using the measurements the module parameters are calculated using least square curve fitting method. PV array model is developed using Lambert-W function and is implemented for different configurations.

A C-language based method is proposed in [161] in which an R_s model is considered for simulation. The value diode ideality factor is selected as cubic dependence of temperature given by Eq. (44).

$$I_o = aT^3 \exp\left(\frac{-E_g}{KT}\right) \quad (44)$$

The program coded in C is implemented in visual C++ platform using numerical analysis for partial shading condition.

A model with single diode model for mismatched PV fields by means of Lambert-W function is presented in [162]. The output current is expressed explicitly as a function of voltage using Lambert-W function. The model is expressed in terms of $(N+1)$ equations with equal number of unknowns $\{V_1, V_2,\ldots, V_N, V_{diode}\}$ with which one voltage equation and six current equations can be obtained. The current equations are obtained by

$$I_k(V_k) - I_{k-1}(V_{k-1}) = 0 \quad (45)$$

where the value of *k* varies from 2 to $(N+1)$. This is obtained because all the modules are connected in series where the current is same. With the obtained set of seven, Newton Raphson method is used for obtaining the string current by expressing it in terms of Jacobian matrix. A detailed model of bypass and blocking diode is presented.

A simplified version of [162] is presented in [163]. The approximations used are neglecting series and shunt resistances, and bypass diode is modeled as an ideal switch. A set of non-linear equations that describes PV field in both uniform and non-uniform irradiances is presented. An optimized Newton Raphson method is used for speeding up the numerical procedure. The model is simple and less accurate and is used for predicting the PV array performance under non-uniform irradiance conditions for a long term evaluations of energy on a daily, monthly and yearly basis. An extension to [163] is presented in [165] for bridge linked configuration. Ideal diode model is used. Schokley diode is used for modeling bypass diode.

The method presented in [164] is an improved version of [162]. A single diode model is considered with detailed modeling of bypass diodes. An extension of work done in [164] is presented in [166] which used Schur compliment for obtaining the inverse Jacobian matrix. The modeling is done at cell level using the model in [4].

Table 10
Comparison of iterative methods.

#	Authors	Ref.	Type	Par.	Diode	Contribution
1	Quaschning et al. (1996)	[156]	1D	5	D	Numerical analysis is performed
2	Nguyen et al. (2006)	[157]	1D	5	D	Extended [156] to various configurations
3	Ishaque et al. (2011a)	[158]	2D	4	P	Extended [51] to non-uniform irradiance using linear interpolation
4	Ishaque et al. (2011b)	[159]	2D	4	P	Implemented [158] in simulink
5	Picault et al. (2010)	[160]	1D	5	P	Based on field measurements and curve fitting
13	Ji et al. (2009)	[160]	R_s	4	D	Implemented using C
6	Petrone et al. (2007)	[162]	1D	5	D	Implemented Lambert-W function with Jacobian matrix and solved using NR methods
7	Petrone et al. (2011)	[163]	ID	3	I	Simplified [162], compromising accuracy and increasing speed
8	Orozco et al. (2013)	[164]	ID	3	I	Implemented [163] using Schur complement in inverse Jacobian matrix
9	Batidas et al. (2013)	[165]	ID	3	I	Implemented bridge linked configuration using [163]
10	Orozco et al. (2014)	[166]	1D	7	I	Extended [164] and implemented cell level study using [163]
11	Ramos Paja et al. (2012)	[167]	ID	3	I	Extended [163] for TCT
12	Batidas et al. (2013)	[168]	1D	5	P	Trade-off between [162,163]
13	Bastidas et al. (2013)	[169]	ID	3	P	Used trust region algorithm
14	Kadri et al. (2012)	[170]	1D	5	I	Based on matrices
15	Diaz et al. (2014)	[171]	1D	7	D	Discretized model of [4]
22	Wang et al. (2011)	[17]	1D	7	D	PLPB in uniform irradiance is extended for non-uniform irradiance using PSIM or EMTP

D: detailed model of bypass diode; P: piece wise linear model of bypass diode; I: ideal model of bypass diode.

Table 11
Comparison of artificial intelligence methods.

#	Authors	Ref.	Type	Par.	Diode	Contribution
1	Ismail et al. (2013)	[77]	1D	5	P	Based on GA
2	Karapete et al. (2007)	[172]	1D	5	D	Based on ANN
3	Fathy (2015)	[173]	1D	5	P	Based on ABC
4	Lun et al. (2014)	[126]	1D	5	P	Based on time wrap invariant echo state network

A mathematical procedure for modeling TCT configuration (N rows with M modules each) is presented in [167]. An ideal diode is considered with three parameters. Light generated current is approximated as short circuit current. The formation of equations for obtaining row current is similar to procedure given in [162] where the modules are connected in series. But in a row, the modules are connected in parallel. The necessary alterations are made and once the row current is computed, entire array current is found using the same procedure in [162] because all the rows are connected in series.

A trade-off model that comprises the advantages of [162,163] is proposed in [168]. A single diode model is considered. Blocking and bypass diodes are considered as piecewise linear models. Output voltage is expressed as an explicit function of current using lambert-W function. Unlike [162,163] no matrix is used. The entire set of PV voltages of modules connected in a string and is expressed in a single equation which contains the expressions for voltage of active modules, inactive modules (bypass diodes) and voltage of blocking diodes. Once the expression of string voltage is obtained, Newton Raphson method is used to obtain the value of string current.

A method based on Trust region algorithm that uses experimental data to find the model parameters is presented in [169]. An ideal diode model is considered. Blocking diodes and bypass diodes are modeled as piecewise linear model. A term point of interest is introduced which consists of OCP, SCP, and inflection points (point where step occurs in the I–V curve). The parameters are determined from the experimental data based on nonlinear squares method and trust region algorithm is used to determine the parameters. Four steps are involved in finding the parameters. First, the parameters are initialized. Second the curve is fitted for set of parameters. Third, adjustment of parameters and checked whether fitting is improved or not. Finally, if fit is not improved the direction and magnitude of parameters are adjusted using trust region algorithm.

A single diode model to analyze the effects of non-uniform irradiance is presented in [170]. This model presented a set of matrix equations to describe the PV behavior. Each type of cell connection is considered. The equivalent circuit parameters and MPP of PV system are calculated. In order to validate the behavior of PV array, a real time emulator based on closed loop reference model is used.

A discrete I–V model for partially shaded PV arrays is proposed in [171]. This method is based on Bishops model presented in [4]. PV system is modeled by discretizing the currents and voltages of PV cells. Newton Raphson method, analytical approximation and interpolation methods are used to obtain the relation between discrete currents and voltages. In order to avoid solving large system of non-linear equations, the discrete model is developed, which is an improvement, generalization and systematization of the one introduced in [4]. Bypass diodes are used where the current and voltage of it are discretized.

A piecewise linear parallel branch model (PLPB) is proposed in [17] for non-uniform irradiance. In this paper the parameters are solved using NR method. The model is implemented for different topologies viz., SS, SP, TCT, HB and is implemented in circuit simulator software such as PSIM or EMTP (Table 10).

3.3. Artificial intelligence based methods

A method based on genetic algorithm is presented in [77]. The results obtained are compared with an ANN based emulator. A single diode model is considered to model the PV system under non-uniform irradiance in [172]. An artificial neural network is used to find the five equivalent circuit parameters. Once the five equivalent circuit parameters are found, the bypass diodes and blocking diodes are modeled. A method of modeling based on ABC algorithm is presented in [173]. The original ABC algorithm is modified so as to accelerate the solution and to converge to global optimized one. A method based on time-wrap invariant echo state network is presented in [126] for a two diode model. Real operating data is used for modifying the PV arrays in order to make it robust for various environmental conditions (Table 11).

Table 12
Comparison of different modeling techniques in uniform irradiance conditions.

Type of irradiance	Methods	Perturbation	Complexity	Accuracy	Speed
Uniform irradiance	Non-iterative methods	No	L	L	L
	Iterative methods	F and A	H	H	M
	Artificial intelligence techniques	A	VH	VH	H
	Dynamic models	A	VH	VH	VH
Non-uniform irradiance	Non-iterative methods	No	L	L	L
	Iterative methods	F and A	VH	H	M
	Artificial intelligence techniques	A	VH	VH	L

4. Comparison of modeling techniques

Classification of modeling techniques is based on type of model, number of equivalent circuit parameters used, method used for solving to obtain the equivalent circuit diagrams, perturbation of the model, implementation complexity, accuracy, computational speed, type of bypass/blocking diode.

4.1. According to perturbation of parameters

In most of the methods the parameters need to be perturbed. There are two types perturbation fixed (F) and adaptive (A). In some methods there is no need to perturb the parameters.

4.2. According to implementation complexity

These are divided into five groups: very less (VL), less (L), moderate (M), high (H), very high (VH).

4.3. According to accuracy

These are divided into five groups: very less (VL), less (L), moderate (M), high (H), very high (VH).

4.4. According to computational speed

These are divided into five groups: very less (VL), less (L), moderate (M), high (H), very high (VH). Table 12 presents the comparison in uniform irradiance conditions and non-uniform irradiance conditions.

5. Conclusion

The article presented in this paper reviewed the modeling techniques of uniform and non-uniform irradiance conditions separately. A classifications of uniform and non-uniform methods are done based on type of model, equivalent circuit used, number of equivalent circuit parameters, method used for modeling equivalent circuit parameters, perturbation of parameters, implementation complexity, accuracy, and speed. Apart from this another classification is used for non-uniform irradiance i.e., type of bypass diode. It is expected that this review can be a useful reference for researchers who want to work on modeling of PV systems in both uniform and non-uniform irradiance conditions.

References

[1] Villalva MG, Gazoli JR. Comprehensive approach to modeling and simulation of photovoltaic arrays. IEEE Trans Power Electron 2009;24(5):1198–208.
[2] Nishioka K, Sakitani N, Uraoka Y, Fuyuki T. Analysis of multi crystalline silicon solar cells by modified 3-diode equivalent circuit model taking leakage current through periphery into consideration. Sol Energy Mater Sol Cells 2007;91(13):1222–7.
[3] Kim KA, Xu C, Jin L, Krein PT. a dynamic photovoltaic model incorporating capacitive and reverse-bias characteristics. IEEE J Photovolt 2013;3(4):1334–41.
[4] Bishop JW. Computer simulation of the effects of electrical mismatches in photovoltaic cell interconnection circuits. Sol cells 1988;25(1):73–89.
[5] Cotfas DT, Cotfas PA, Kaplanis S. Methods to determine the dc parameters of solar cells: a critical review. Renew Sustain Energy Rev 2013;28:588–96.
[6] Phang JCH, Chan DSH, Phillips JR. Accurate analytical method for the extraction of solar cell model parameters. Electron Lett 1984;20(10):406–8.
[7] Chan DS, Phang JC. Analytical methods for the extraction of solar-cell single- and double-diode model parameters from *I–V* characteristics. IEEE Trans Electron Devices 1987;34(2):286–93.
[8] Walker G. Evaluating MPPT converter topologies using a MATLAB PV model. J Electr Electron Eng 2001;21(1):49–56.
[9] Tsai HL, Tu CS, Su YJ. Development of generalized photovoltaic model using MATLAB/SIMULINK. In: Proceedings of the world congress on Engineering and computer science; 2008. p. 1–6.
[10] Jain A, Kapoor A. Exact analytical solutions of the parameters of real solar cells using Lambert W-function. Sol Energy Mater Sol Cells 2004;81(2):269–77.
[11] Jain A, Kapoor A. A new method to determine the diode ideality factor of real solar cell using Lambert W-function. Sol Energy Mater Sol Cells 2005;85(3):391–6.
[12] Cubas J, Pindado S, de Manuel C. Explicit expressions for solar panel equivalent circuit parameters based on analytical formulation and the Lambert W-function. Energies 2014;7(7):4098–115.
[13] Cubas J, Pindado S, Victoria M. On the analytical approach for modeling photovoltaic systems behavior. J Power Sources 2014;247:467–74.
[14] De Soto W, Klein SA, Beckman WA. Improvement and validation of a model for photovoltaic array performance. Sol Energy 2006;80(1):78–88.
[15] Tian H, Mancilla-David F, Ellis K, Muljadi E, Jenkins P. A cell-to-module-to-array detailed model for photovoltaic panels. Sol Energy 2012;86(9):2695–706.
[16] Azab M. Improved circuit model of photovoltaic array. Int J Electr Power Energy Syst Eng 2009;2(3):185–8.
[17] Wang YJ, Hsu PC. An investigation on partial shading of PV modules with different connection configurations of PV cells. Energy 2011;36(5):3069–78.
[18] Bellini A, Bifaretti S, Iacovone V, Cornaro C. Simplified model of a photovoltaic module. In: Proceedings of the IEEE Applied Electronics; 2009. p. 47–51.
[19] Chakrasali RL, Sheelavant VR, Nagaraja HN. Network approach to modeling and simulation of solar photovoltaic cell. Renew Sustain Energy Rev 2013;21:84–8.
[20] Saloux E, Teyssedou A, Sorin M. Explicit model of photovoltaic panels to determine voltages and currents at the maximum power point. Sol Energy 2011;85(5):713–22.
[21] MassiPavan A, Mellit A, Lughi V. Explicit empirical model for general photovoltaic devices: experimental validation at maximum power point. Sol Energy 2014;101:105–16.
[22] Chouder A, Silvestre S, Sadaoui N, Rahmani L. Modeling and simulation of a grid connected PV system based on the evaluation of main PV module parameters. Simul Model Pract Theory 2012;20(1):46–58.
[23] Xiao W, Edwin FF, Spagnuolo G, Jatskevich J. Efficient approaches for modeling and simulating photovoltaic power systems. IEEE J Photovolt 2013;3(1):500–8.
[24] Di Vincenzo MC, Infield D. Detailed PV array model for non-uniform irradiance and its validation against experimental data. Sol Energy 2013;97:314–31.
[25] Rahman SA, Varma RK, Vanderheide T. Generalised model of a photovoltaic panel. IET Renew Power Gener 2014;8(3):217–29.
[26] Bai J, Liu S, Hao Y, Zhang Z, Jiang M, Zhang Y. Development of a new compound method to extract the five parameters of PV modules. Energy Convers Manag 2014;79:294–303.
[27] Toledo FJ, Blanes JM. Geometric properties of the single-diode photovoltaic model and a new very simple method for parameters extraction. Renew Energy 2014;72:125–33.
[28] Khezzar R, Zereg M, Khezzar A. Modeling improvement of the four parameter model for photovoltaic modules. Sol Energy 2014;110:452–62.

[29] Kennerud KL. Analysis of performance degradation in CdS solar cells. IEEE Trans Aerosp Electron Syst 1969;6:912–7.
[30] Easwarakhanthan T, Bottin J, Bouhouch I, Boutrit C. Nonlinear minimization algorithm for determining the solar cell parameters with microcomputers. Int J Sol Energy 1986;4(1):1–12.
[31] Gow JA, Manning CD. Development of a model for photovoltaic arrays suitable for use in simulation studies of solar energy conversion systems. In: Proceedings of the sixth international conference on power electronics and variable speed drives; 1996. p. 69–74.
[32] Gow JA, Manning CD. Development of a photovoltaic array model for use in power-electronics simulation studies. IET Electric Power Appl 1999;146 (2):193–200.
[33] Chowdhury S, Taylor GA, Chowdhury SP, Saha AK, Song YH. Modelling, simulation and performance analysis of a PV array in an embedded environment. In: Proceedings of IEEE 42nd International Universities Power Engineering Conference; 2007. p. 781–5.
[34] Nakanishi F, Ikegami T, Ebihara K, Kuriyama S, Shiota Y. Modeling and operation of a 10 kW photovoltaic power generator using equivalent electric circuit method. In: Proceedings of IEEE 28th Photovoltaic Specialists Conference; 2000. p. 1703–6.
[35] Gottschalg R, Rommel M, Infield DG, Kearney MJ. The influence of the measurement environment on the accuracy of the extraction of the physical parameters of solar cells. Meas Sci Technol 1999;10(9):796.
[36] Dkhichi F, Oukarfi B, Fakkar A, Belbounaguia N. Parameter identification of solar cell model using Levenberg–Marquardt algorithm combined with simulated annealing. Sol Energy 2014;110:781–8.
[37] Bouzidi K, Chegaar M, Bouhemadou A. Solar cells parameters evaluation considering the series and shunt resistance. Sol Energy Mater Sol Cells 2007;91(18):1647–51.
[38] Tossa AK, Soro YM, Azoumah Y, Yamegueu D. A new approach to estimate the performance and energy productivity of photovoltaic modules in real operating conditions. Sol Energy 2014;110:543–60.
[39] Ma T, Yang H, Lu L. Development of a model to simulate the performance characteristics of crystalline silicon photovoltaic modules/strings/arrays. Sol Energy 2014;100:31–41.
[40] Ma T, Yang H, Lu L. Solar photovoltaic system modeling and performance prediction. Renew Sustain Energy Rev 2014;36:304–15.
[41] Chegaar M, Ouennoughi Z, Guechi F. Extracting dc parameters of solar cells under illumination. Vacuum 2004;75(4):367–72.
[42] Ortiz-Conde A, García Sánchez FJ, Muci J. New method to extract the model parameters of solar cells from the explicit analytic solutions of their illuminated *I–V* characteristics. Sol Energy Mater Sol Cells 2006;90 (3):352–61.
[43] Xiao W, Dunford WG, Capel A. A novel modeling method for photovoltaic cells. In: Proceedings of the IEEE 35th Annual Power Electronics Specialists Conference; 2004. p. 1950–6.
[44] Sera D, Teodorescu R., Rodriguez P. PV panel model based on datasheet values. In: Proceedings of the IEEE International Symposium on Industrial Electronics; 2007. p. 2392–6.
[45] Chatterjee A, Keyhani A, Kapoor D. Identification of photovoltaic source models. IEEE Trans Energy Convers 2007;26(3):883–9.
[46] Chatterjee A, Keyhani A. Thevenin's equivalent of photovoltaic source models for MPPT and power grid studies. In: Proceedings of the IEEE Power and Energy Society General Meeting; 2011. p. 1–7.
[47] Can H, Ickilli D. Parameter estimation in modeling of photovoltaic panels based on datasheet values. J Sol Energy Eng 2014;136:2.
[48] Hejri M, Mokhtari H, Azizian MR, Ghandhari M, Soder L. On the parameter extraction of a five-parameter double-diode model of photovoltaic cells and modules. IEEE J Photovolt 2014;4(3):915–23.
[49] Petreuş D, Fărcaş C, Ciocan I. Modelling and simulation of photovoltaic cells. ActaNapocensis—Electron Telecommun 2008;49(1):42–7.
[50] Ishaque K, Salam Z, Taheri H. Simple, fast and accurate two-diode model for photovoltaic modules. Sol Energy Mater Sol Cells 2011;95(2):586–94.
[51] Ishaque K, Salam Z, Taheri H. Accurate MATLAB simulink PV system simulator based on a two-diode model. J Power Electronics 2011;11 (2):179–87.
[52] Jena D, Ramana VV. An accurate modeling of photovoltaic system for uniform and non-uniform irradiance. Int J Renew Energy Res (IJRER) 2015;5(1):29–40.
[53] Babu BC, Gurjar S. A novel simplified two-diode model of photovoltaic (PV) module. IEEE J Photovolt 2014;4(4):1156–61.
[54] Ghani F, Duke M. Numerical determination of parasitic resistances of a solar cell using the Lambert W-function. Sol Energy 2011;85(9):2386–94.
[55] Ghani F, Rosengarten G, Duke M, Carson JK. The numerical calculation of single-diode solar-cell modelling parameters. Renew Energy 2014;72:105–12.
[56] Ghani F, Rosengarten G, Duke M, Carson JK. On the influence of temperature on crystalline silicon solar cell characterization parameters. Sol Energy 2015;112:437–45.
[57] Kong KC, bin Mamat M, Ibrahim MZ, Muzathik AM. New approach on mathematical modeling of photovoltaic solar panel. Appl Math Sci 2012;6 (8):381–401.
[58] AlHajri MF, El-Naggar KM, AlRashidi MR, Al-Othman AK. Optimal extraction of solar cell parameters using pattern search. Renew Energy 2012;44:238–45.
[59] AlRashidi MR, AlHajri MF, El-Naggar KM, Al-Othman AK. A new estimation approach for determining the *I–V* characteristics of solar cells. Sol Energy 2011;85(7):1543–50.
[60] Caracciolo F, Dallago E, Finarelli DG, Liberale A, Merhej P. Single-variable optimization method for evaluating solar cell and solar module parameters. IEEE J Photovolt 2012;2(2):173–80.
[61] Cannizzaro S, Di Piazza MC, Luna M, Vitale G. Generalized classification of PV modules by simplified single-diode models. In: Proceedings of IEEE 23rd International Symposium on Industrial Electronics (ISIE); 2014 p. 2266–73.
[62] Xu Y, Kong X, Zeng Y, Tao S, Xiao X. A modeling method for photovoltaic cells using explicit equations and optimization algorithm. Int J Electr Power Energy Syst 2014;59:23–8.
[63] Zhang K, Jia W, Koplowitz J, Marzocca P, Cheng MC. Modeling of photovoltaic cells and arrays based on singular value decomposition. Semicond Sci Technol 2013;28(3):035002.
[64] Mahmoud YA, Xiao W, Zeineldin HH. A parameterization approach for enhancing PV model accuracy. IEEE Trans Ind Electron 2013;60(12):5708–16.
[65] Laudani A, Mancilla-David F, Riganti-Fulginei F, Salvini A. Reduced-form of the photovoltaic five-parameter model for efficient computation of parameters. Sol Energy 2013;97:122–7.
[66] Laudani A, Fulginei FR, Salvini A. High performing extraction procedure for the one-diode model of a photovoltaic panel from experimental *I–V* curves by using reduced forms. Sol Energy 2014;103:316–26.
[67] Laudani A, Fulginei FR, Salvini A. Identification of the one-diode model for photovoltaic modules from datasheet values. Sol Energy 2014;108:432–46.
[68] Elbaset AA, Ali H, Abd-El Sattar M. Novel seven-parameter model for photovoltaic modules. Sol Energy Mater Sol Cells 2014;130:442–55.
[69] Peng L, Sun Y, Meng Z. An improved model and parameters extraction for photovoltaic cells using only three state points at standard test condition. J Power Sources 2014;248:621–31.
[70] Lim L, Ye Z, Ye J, Yang D, Du H. A linear identification of diode models from single IV characteristics of PV panels. IEEE Trans Ind Electron 2015;62 (7):4181–93.
[71] Ding K, Zhang J, Bian X, Xu J. A simplified model for photovoltaic modules based on improved translation equations. Sol Energy 2014;101:40–52.
[72] Lineykin S, Averbukh M, Kuperman A. An improved approach to extract the single-diode equivalent circuit parameters of a photovoltaic cell/panel. Renew Sustain Energy Rev 2014;30:282–9.
[73] Moldovan N, Picos R, Garcia-Moreno E. Parameter extraction of a solar cell compact model using genetic algorithms. In: Proceedings of IEEE Spanish Conference on Electron Devices; 2009. p. 379–82.
[74] Jervase JA, Bourdoucen H, Al-Lawati A. Solar cell parameter extraction using genetic algorithms. Meas Sci Technol 2001;12(11):1922.
[75] Zagrouba M, Sellami A, Bouaïcha M, Ksouri M. Identification of PV solar cells and modules parameters using the genetic algorithms: application to maximum power extraction. Sol Energy 2010;84(5):860–6.
[76] Lingyun X, Lefei S, Wei H, Cong J. Solar cells parameter extraction using a hybrid genetic algorithm. In: Proceedings of Third International Conference on Measuring Technology and Mechatronics Automation (ICMTMA); 2011. p. 306–9.
[77] Ismail MS, Moghavvemi M, Mahlia TMI. Characterization of PV panel and global optimization of its model parameters using genetic algorithm. Energy Convers Manag 2013;73:10–25.
[78] Appelbaum J, Peled A. Parameters extraction of solar cells—a comparative examination of three methods. Sol Energy Mater Sol Cells 2014;122:164–73.
[79] Dizqah AM, Maheri A, Busawon K. An accurate method for the PV model identification based on a genetic algorithm and the interior-point method. Renew Energy 2014;72:212–22.
[80] Qin H, Kimball JW. Parameter determination of photovoltaic cells from field testing data using particle swarm optimization. In: Proceedings of IEEE Power and Energy Conference at Illinois (PECI); 2011. p. 1–4.
[81] Wang X. M, Xu Y. Parameter extraction of solar cells using particle swarm optimization. J Appl Phys 2009;105(9):094502.
[82] Ye M, Zeng S, Xu Y. An extraction method of solar cell parameters with improved particle swarm optimization. ECS Trans 2010;27(1):1099–104.
[83] Wei H, Cong J, Lingyun X, Deyun S. Extracting solar cell model parameters based on chaos particle swarm algorithm. In: Proceedings of IEEE International Conference on Electric Information and Control Engineering (ICEICE); 2011. p. 398–402.
[84] Macabebe EQB, Sheppard CJ, van Dyk EE. Parameter extraction from I-V characteristics of PV devices. Sol Energy 2011;85(1):12–8.
[85] Sandrolini L, Artioli M, Reggiani U. Numerical method for the extraction of photovoltaic module double-diode model parameters through cluster analysis. Appl Energy 2010;87(2):442–51.
[86] Soon JJ, Low KS. Photovoltaic model identification using particle swarm optimization with inverse barrier constraint. IEEE Trans Power Electron 2012;27(9):3975–83.
[87] Hamid A, Farhana N, Rahim NA, Selvaraj J. Solar cell parameters extraction using particle swarm optimization algorithm. In: Proceedings of IEEE Conference on Clean Energy and Technology (CEAT); 2013. p. 461–5.
[88] Khanna V, Das BK, Bisht D, Singh PK. A three diode model for industrial solar cells and estimation of solar cell parameters using PSO algorithm. Renew Energy 2015;78:105–13.
[89] Soon JJ, Low KS. Optimizing photovoltaic model for different cell technologies using a generalized multi-dimension diode model. IEEE Trans Ind Electron 2015. http://dx.doi.org/10.1109/TIE.2015.2420617.
[90] da Costa WT, Fardin JF, Simonetti DS, Neto L.Identification of photovoltaic model parameters by differential evolution. In: Proceedings of IEEE International Conference on Industrial Technology (ICIT); 2010. p. 931–6.

[91] Ishaque K, Salam Z, Mekhilef S, Shamsudin A. Parameter extraction of solar photovoltaic modules using penalty-based differential evolution. Appl Energy 2012;99:297–308.
[92] Ishaque K, Salam Z. An improved modeling method to determine the model parameters of photovoltaic (PV) modules using differential evolution (DE). Sol Energy 2011;85(9):2349–59.
[93] Ishaque K, Salam Z, Taheri H, Shamsudin A. A critical evaluation of EA computational methods for photovoltaic cell parameter extraction based on two diode model. Sol Energy 2011;85(9):1768–79.
[94] Gong W, Cai Z. Parameter extraction of solar cell models using repaired adaptive differential evolution. Sol Energy 2013;94:209–20.
[95] Jiang LL, Maskell DL, Patra JC. Parameter estimation of solar cells and modules using an improved adaptive differential evolution algorithm. Appl Energy 2013;112:185–93.
[96] Asif S, Li Y. Solar cell modeling and parameter optimization using simulated annealing. J Propuls Power 2008;24(5):1018–22.
[97] El-Naggar KM, AlRashidi MR, AlHajri MF, Al-Othman AK. Simulated annealing algorithm for photovoltaic parameters identification. Sol Energy 2012;86(1):266–74.
[98] Ma J, Ting TO, Man KL, Zhang N, Guan SU, Wong PW. Parameter estimation of photovoltaic models via cuckoo search. J Appl Math 2013; Article ID: 362619, 1-8.
[99] Siddiqui MU, Abido M. Parameter estimation for five-and seven-parameter photovoltaic electrical models using evolutionary algorithms. Appl Soft Comput 2013;13(12):4608–21.
[100] Askarzadeh A, Rezazadeh A. Extraction of maximum power point in solar cells using bird mating optimizer-based parameters identification approach. Sol Energy 2013;90:123–33.
[101] Askarzadeh A, dos Santos Coelho L. Determination of photovoltaic modules parameters at different operating conditions using a novel bird mating optimizer approach. Energy Convers Manag 2015;89:608–14.
[102] Askarzadeh A, Rezazadeh A. Artificial bee swarm optimization algorithm for parameters identification of solar cell models. Appl Energy 2013;102:943–9.
[103] Oliva D, Cuevas E, Pajares G. Parameter identification of solar cells using artificial bee colony optimization. Energy 2014;72:93–102.
[104] Hasanien HM. Shuffled frog leaping algorithm for photovoltaic model identification. IEEE Trans Sustain Energy 2015;6(2):509–15.
[105] Askarzadeh A, Rezazadeh A. Parameter identification for solar cell models using harmony search-based algorithms. Sol Energy 2012;86(11):3241–9.
[106] Han W, Wang HH, Chen L. Parameters identification for photovoltaic module based on an improved artificial fish swarm algorithm. Sci World J 2014.
[107] Niu Q, Zhang H, Li K. An improved TLBO with elite strategy for parameters identification of PEM fuel cell and solar cell models. Int J Hydrog Energy 2014;39(8):3837–54.
[108] Patel SJ, Panchal AK, Kheraj V. Extraction of solar cell parameters from a single current–voltage characteristic using teaching learning based optimization algorithm. Appl Energy 2014;119:384–93.
[109] Niu Q, Zhang L, Li K. A biogeography-based optimization algorithm with mutation strategies for model parameter estimation of solar and fuel cells. Energy Convers Manag 2014;86:1173–85.
[110] Ji M, Jin Z, Tang H. An improved simulated annealing for solving the linear constrained optimization problems. Appl Math Comput 2006;183(1):251–9.
[111] Elshatter TF, Elhagry MT, Abou-Elzahab EM, Elkousy AAT. Fuzzy modeling of photovoltaic panel equivalent circuit. In: Proceedings of IEEE 28th Photovoltaic Specialists Conference; 2000. p. 1656–9.
[112] Balzani M., Reatti A. Neural network based model of a PV array for the optimum performance of PV system. In: Proceedings of IEEE Research in Microelectronics and Electronics, vol. 2; 2005. p. 123–6.
[113] Karatepe E, Boztepe M, Colak M. Neural network based solar cell model. Energy Convers Manag 2006;47(9):1159–78.
[114] Celik AN. Artificial neural network modelling and experimental verification of the operating current of mono-crystalline photovoltaic modules. Sol Energy 2011;85(10):2507–17.
[115] Almonacid F, Rus C, Hontoria L, Fuentes M, Nofuentes G. Characterisation of Si-crystalline PV modules by artificial neural networks. Renew Energy 2009;34(4):941–9.
[116] Karamirad M, Omid M, Alimardani R, Mousazadeh H, Heidari SN. ANN based simulation and experimental verification of analytical four-and five-parameter models of PV modules. Simul Model Pract Theory 2013;34:86–98.
[117] Ramaprabha R, Mathur BL, Sharanya M. Solar array modeling and simulation of MPPT using neural network. In: Proceedings of IEEE International Conference on Control, Automation, Communication and Energy Conservation; 2009. p. 1–5.
[118] Bonanno F, Capizzi G, Graditi G, Napoli C, Tina GM. A radial basis function neural network based approach for the electrical characteristics estimation of a photovoltaic module. Appl Energy 2012;97:956–61.
[119] Chikh A, Chandra A. Adaptive neuro-fuzzy based solar cell model. IET Renew Power Gener 2014;8(6):679–86.
[120] Fathabadi H. Novel neural-analytical method for determining silicon/plastic solar cells and modules characteristics. Energy Convers Manag 2013;76:253–9.
[121] Kulaksiz AA. ANFIS-based estimation of PV module equivalent parameters: application to a stand-alone PV system with MPPT controller. Turk J Electr Eng Comput Sci 2013;21(2):2127–40.
[122] Laudani A, Lozito, GM, Riganti Fulginei F, Salvini A. Hybrid neural network approach based tool for the modelling of photovoltaic panels. Int J Photoenergy 2015; Article ID: 413654, 1-10.
[123] Madden GJ, Le A. Solar panel model for design and analysis of power regulation equipment. In: Proceedings of AIAA; 1994. p. 151–6.
[124] Kumar RA, Suresh MS, Nagaraju J. Silicon (BSFR) solar cell AC parameters at different temperatures. Sol Energy Mater Sol Cells 2005;85(3):397–406.
[125] Di Piazza MC, Luna M, Vitale G. Dynamic PV model parameter identification by least-squares regression. IEEE J Photovolt 2013;3(2):799–806.
[126] Lun SX, Wang S, Guo TT, Du CJ. An I–V model based on time warp invariant echo state network for photovoltaic array with shaded solar cells. Sol Energy 2014;105:529–41.
[127] Kawamura H, Naka K, Yonekura N, Yamanaka S, Kawamura H, Ohno H, et al. Simulation of I-V characteristics of a PV module with shaded PV cells. Sol Energy Mater Sol Cells 2003;75(3):613–21.
[128] Alonso-Garcia MC, Ruiz JM, Chenlo F. Experimental study of mismatch and shading effects in the I–V characteristic of a photovoltaic module. Sol Energy Mater Sol Cells 2006;90(3):329–40.
[129] Alonso-Garcia MC, Ruiz JM, Herrmann W. Computer simulation of shading effects in photovoltaic arrays. Renew Energy 2006;31(12):1986–93.
[130] Batzelis EI, Routsolias IA, Papathanassiou SA. An explicit PV string model based on the Lambert function and simplified MPP expressions for operation under partial shading. IEEE Trans Sustain Energy 2014;5(1):301–12.
[131] Psarros GN, Batzelis E, Papathanassiou S. Partial shading analysis of multi-string PV arrays and derivation of simplified MPP expressions. Sustain IEEE Trans Energy 2015;6(2):499–508.
[132] Besheer AH, Kassem AM, Abdelaziz AY. Single-diode model based photovoltaic module: analysis and comparison approach. Electric Power Compon Syst 2014;42(12):1289–300.
[133] Paraskevadaki EV, Papathanassiou SA. Evaluation of MPP voltage and power of mc-Si PV modules in partial shading conditions. IEEE Trans Energy Convers 2011;26(3):923–32.
[134] Patel H, Agarwal V. MATLAB-based modeling to study the effects of partial shading on PV array characteristics. IEEE Trans Energy Convers 2008;23(1):302–10.
[135] Bays N, Clifton J, Hatipoglu K. MATLAB-Graphical User Interface to study partial shading of PV array characteristics. In: Proceedings of IEEE SOUTHEASTCON; 2014. p. 1–4.
[136] Paasch KM, Nymand M, Kjaer SB. Simulation of the impact of moving clouds on large scale PV-plants. In: Proceedings of 40th IEEE Photovoltaic Specialist Conference (PVSC); 2014. p. 0791–6.
[137] Yi Y, Sheng-lan J, Hai-qin G, Juan C. Simulation study on characteristics of photovoltaic array under partial shading. In: Proceedings of IEEE 33rd Chinese Control Conference (CCC); 2014. p. 6992–7.
[138] Wang YJ, Hsu PC. Analytical modelling of partial shading and different orientation of photovoltaic modules. IET Renew Power Gener 2010;4(3):272–82.
[139] Ramabadran R, Mathur B. Effect of shading on series and parallel connected solar PV modules. Mod Appl Sci 2009;3(10):32.
[140] Ramaprabha R, Mathur BL. Modelling and simulation of solar PV array under partial shaded conditions. In: Proceedings of IEEE International Conference on Sustainable Energy Technologies; 2008. p. 7–11.
[141] Ramaprabha R, Mathur BL. MATLAB based modelling to study the influence of shading on series connected SPVA. In: Proceedings of 2nd IEEE International Conference on Emerging Trends in Engineering and Technology (ICETET); 2009. p. 30–4.
[142] Ding K, Bian X, Liu H, Peng T. A MATLAB-simulink-based PV module model and its application under conditions of non uniform irradiance. IEEE Trans Energy Convers 2012;27(4):864–72.
[143] Alajmi BN, Ahmed KH, Finney SJ, Williams BW. A maximum power point tracking technique for partially shaded photovoltaic systems in microgrids. IEEE Trans Ind Electronics 2013;60(4):1596–606.
[144] MassiPavan A, Mellit A, De Pieri D, Lughi V. A study on the mismatch effect due to the use of different photovoltaic modules classes in large-scale solar parks. Prog Photovolt: Res Appl 2012.
[145] Lun SX, Wang S, Yang GH, Guo TT. A new explicit double-diode modeling method based on Lambert W-function for photovoltaic arrays. Sol Energy 2015;116:69–82.
[146] d'Alessandro V, Guerriero P, Daliento S. A simple bipolar transistor-based bypass approach for photovoltaic modules. IEEE J Photovolt 2014;4(1):405–13.
[147] Guo S, Walsh TM, Aberle AG, Peters M. Analysing partial shading of PV modules by circuit modelling. In: Proceedings of 38th IEEE Photovoltaic Specialists Conference (PVSC); p. 002957–60.
[148] Guerrero J, Muñoz Y, Ibáñez F, Ospino A. Analysis of mismatch and shading effects in a photovoltaic array using different technologies. Proc IOP Conf Ser: Mater Sci Eng 2007;59(1):012007.
[149] Qi J, Zhang Y, Chen Y. Modeling and maximum power point tracking (MPPT) method for PV array under partial shade conditions. Renew Energy 2014;66:337–45.
[150] Olalla C, Deline C, Maksimovic D. Modeling and simulation of conventionally wired photovoltaic systems based on differential power processing SubMIC-enhanced PV modules. In: Proceedings of 15th IEEE Workshop on Control and Modeling for Power Electronics (COMPEL); 2014. p. 1–9.

[151] Rodrigo P, Fernández EF, Almonacid F, Pérez-Higueras PJ. A simple accurate model for the calculation of shading power losses in photovoltaic generators. Sol Energy 2013;93:322–33.
[152] Torres-Lobera D, Valkealahti S. Inclusive dynamic thermal and electric simulation model of solar PV systems under varying atmospheric conditions. Sol Energy 2014;105:632–47.
[153] Khalid MS, Abido MA. A novel and accurate photovoltaic simulator based on seven-parameter model. Electr Power Syst Res 2014;116:243–51.
[154] Seyedmahmoudian M, Mekhilef S, Rahmani R, Yusof R, Renani ET. Analytical modeling of partially shaded photovoltaic systems. Energies 2013;6 (1):128–44.
[155] Restrepo Cuestas BJ, TrejosGrisales LA, Ramos Paja CA. Modeling of PV systems based on inflection points technique considering reverse mode. Tecno LóGicas 2013; Extra(0): 237-248.
[156] Quaschning V, Hanitsch R. Numerical simulation of current–voltage characteristics of photovoltaic systems with shaded solar cells. Sol Energy 1996;56(6):513–20.
[157] Nguyen DD, Lehman B. Modeling and simulation of solar PV arrays under changing illumination conditions. In: Proceedings of IEEE workshops on computers in power electronics; 2006. p. 295–9.
[158] Ishaque K, Salam Z, Taheri H. Modeling and simulation of photovoltaic (PV) system during partial shading based on a two-diode model. Simul Model Pract Theory 2011;19(7):1613–26.
[159] Ishaque K, Salam Z. A comprehensive MATLAB Simulink PV system simulator with partial shading capability based on two-diode model. Sol Energy 2011;85(9):2217–27.
[160] Picault D, Raison B, Bacha S, De La Casa J, Aguilera J. Forecasting photovoltaic array power production subject to mismatch losses. Sol Energy 2010;84 (7):1301–9.
[161] Ji YH, Kim JG, Park SH, Kim JH, Won CY. C-language based PV array simulation technique considering effects of partial shading. In: Proceedings of IEEE International Conference on Industrial Technology; 2009. p. 1–6.
[162] Petrone G, Spagnuolo G, Vitelli M. Analytical model of mismatched photovoltaic fields by means of Lambert W-function. Sol Energy Mater Sol Cells 2007;91(18):1652–7.
[163] Petrone G, Ramos-Paja CA. Modeling of photovoltaic fields in mismatched conditions for energy yield evaluations. Electr Power Syst Res 2011;81 (4):1003–13.
[164] Orozco-Gutierrez ML, Ramirez-Scarpetta JM, Spagnuolo G, Ramos-Paja CA. A technique for mismatched PV array simulation. Renew Energy 2013;55:417–27.
[165] Bastidas Rodriguez JD, Ramos Paja CA, TrejosGrisales LA. Mathematical model of bridge-linked photovoltaic arrays operating under irregular conditions;. Tecno LóGicas 2013; Extra(0): 223-235.
[166] Orozco-Gutierrez ML, Ramirez-Scarpetta JM, Spagnuolo G, Ramos-Paja CA. A method for simulating large PV arrays that include reverse biased cells. Appl Energy 2014;123:157–67.
[167] Ramos-Paja CA, Bastidas JD, Saavedra-Montes AJ, Guinjoan-Gispert F, Goez M. Mathematical model of total cross-tied photovoltaic arrays in mismatching conditions. In: Proceedings of IEEE 4th Colombian Workshop on Circuits and Systems (CWCAS); 2012. p. 1–6.
[168] Bastidas JD, Franco E, Petrone G, Ramos-Paja CA, Spagnuolo G. A model of photovoltaic fields in mismatching conditions featuring an improved calculation speed. Electr Power Syst Res 2013;96:81–90.
[169] Bastidas-Rodriguez JD, Ramos-Paja CA, Saavedra-Montes AJ. Reconfiguration analysis of photovoltaic arrays based on parameters estimation. Simul Model Pract Theory 2013;35:50–68.
[170] Kadri R, Andrei H, Gaubert JP, Ivanovici T, Champenois G, Andrei P. Modeling of the photovoltaic cell circuit parameters for optimum connection model and real-time emulator with partial shadow conditions. Energy 2012;42 (1):57–67.
[171] Díaz-Dorado E, Cidrás J, Carrillo C. Discrete *I–V* model for partially shaded PV-arrays. Sol Energy 2014;103:96–107.
[172] Karatepe E, Boztepe M, Colak M. Development of a suitable model for characterizing photovoltaic arrays with shaded solar cells. Sol Energy 2007;81(8):977–92.
[173] Fathy A. Reliable and efficient approach for mitigating the shading effect on photovoltaic module based on Modified Artificial Bee Colony algorithm. Renew Energy 2015;81:78–88.